Universität Bonn

Forschungszentrum Jülich

Study of Exotic Hadrons with Lattice QCD and Distillation

Grant Bradley

Dieser Forschungsbericht wurde als Masterarbeit von der
Mathematisch-Naturwissenschaftlichen Fakultät der Universität Bonn angenommen.

Angenommen am:	23.10.2024
1. Gutachter:	Prof. Dr. Stefan Krieg
2. Gutachterin:	Dr. Giovanni Pederiva

Acknowledgements

I would like to thank my advisor Prof. Dr. Stefan Krieg for giving me the opportunity to pursue my PhD in a beautiful topic and country. He provides endless guidance in both the research vocation and how to navigate the problems that arise when moving to a foreign country. His advice in both realms is always just a door-knock or phone call away and has made my adjustment to Germany, and the frustration-laden process of conducting research, all the more smoother.

I also wish to thank Dr. Giovanni Pederiva for his tireless attention to detail with all things programming, the physics "big picture", and advice on how to manage my workflow in an efficient manner. His programming and HPC expertise have been a crucial factor in progressing this project forward. I am indebetted to his patience and suggestions at every step of the way.

I would be remiss to not acknowledge the fruitful discussions with Dr. Evan Berkowitz; His insightful "mini lectures" have illuminated countless deep truths in physics and group theory that were previously unbeknownst to me.

Contents

1 Introduction **1**

2 Hadron Spectroscopy on the Lattice **3**
2.1 Background . . . 3
2.2 Continuum QCD . . . 3
2.2.1 Path integral formulation of QCD . . . 4
2.2.2 Discretization of the Fermion and Gauge Actions . . . 7
2.3 Wilson's Lattice Quantization of Gauge Fields . . . 7
2.4 Two-Point Euclidean Correlation Functions . . . 10
2.4.1 Summary of LQCD Formalism . . . 11
2.5 Gauge Field Smearing . . . 11
2.5.1 Stout Smearing . . . 12
2.6 Distillation Smearing . . . 12
2.7 Contractions . . . 13

3 Computational Considerations **15**
3.1 Lattice Setup . . . 15
3.2 Software Stack for Distillation . . . 16
3.3 Pipeline . . . 16
3.4 Multigrid Methods in LQCD . . . 17
3.4.1 Eigenpairs/Distillation Basis Calculation . . . 18
3.4.2 Calculating Meson Elementals . . . 19
3.4.3 Calculating Perambulators . . . 19
3.5 Cost and Storage of Distillation . . . 20
3.6 Contractions . . . 20
3.7 Ensemble Details . . . 21

4 Interpolating Operators **23**
4.1 Spin on a cubic lattice . . . 23
4.2 Operators on the lattice . . . 24
4.3 Meson operators at zero total momentum . . . 24
4.3.1 Distilled Meson Correlator . . . 25
4.4 Nonlocal meson operators . . . 26
4.4.1 Derivative operators . . . 26

4.5 Meson-Meson Interpolators . . . 28
4.5.1 Distilled Meson-Meson Interpolators . . . 29

5 Mesonic Signal Saturation **31**

6 Conclusion **35**
6.1 Outlook: Towards the Quark Mass Dependence of $T_{cc}(3875)$ . . . 35
6.1.1 Exotic Hadrons in a (very small) nutshell . . . 35
6.2 Conclusion . . . 36

A Appendix **39**
A.1 Group theory in QCD . . . 39
A.2 Gamma matrices . . . 40
A.2.1 `Chroma` Euclidean Dirac Matrices . . . 40

Bibliography **43**

List of Figures **47**

List of Tables **49**

CHAPTER 1

Introduction

Quantum Chromodynamics is the SU(3) gauge field theory governing the strong force, dictating the dynamics of quarks and gluons. One can have two or three quark states, mesons and baryons, respectively, bound together by gluons. QCD phenomena are informed by two main quark correlations: confinement, whereby color forces allow $q, \bar{q}$ to be correlated only into color singlets, and chiral symmetry breaking. The regime in which the coupling constant of the theory α_s is still small, perturbation theory can reliably be used. However, to probe the hadronic world ($\mu \leq 1GeV$), perturbation theory ceases to be a useful tool. By discretizing Minkowski spacetime into Euclidean spacetime, we can calculate the hadron spectrum and other quantities such as matrix elements. This non-perturbative approach is called Lattice QCD (henceforth LQCD), the only systematically improvable and regularization scheme independent method to probe the strong force. The property of quark confinement can be realized in the lattice version of QCD. For more information on the underlying theory, consult [1],[2],[3],[4],[5].

The quark model was proposed by Gell-Mann and Zweig [6][7] as a refined classification scheme for hadrons in which all hadrons are built out of spin-$\frac{1}{2}$ quarks that transform according to the fundamental representation of SU(3). The basic tenants are: There are three flavors of quarks (u, d, s) in the fundamental representation **3**, with their antipartners in the **3***, mesons are $q\bar{q}$ bound states which reside in SU(3) singlets and octets, and that baryons are qqq bound states. This original “simple" quark model contained paradoxes that were resolved by Greenberg, Nambu and others [8] with the introduction of a hidden quark degree of freedom, color; Each quark comes in three differnt colors (red,green,blue) which are packaged in a triplet under a color SU(3) group. This gives rise to the postulate that only color singlet states are physically observable states. Thus, the theory of QCD hinges upon the exchange of gluons between colored quarks.

Hadronic states that do not fit into the traditional quark model have been coined XYZ states [9] or exotics, such as tetraquark and pentaquark states[10]. Multiquark states are posited to be combinations of conventional mesons or diquark-antidiquark pairs, which imply colored building blocks. QCD should predict whether tetraquark states exist, thus, we can leverage the lattice to construct color-flavor-spatial-spin structures resembling that of compact tetraquarks, such as the $T_{cc}^{+}(3875)$, which is the focus of this project. The lack of a consensus as to how the experimental data is to be interpreted, namely the make-up of the aforementioned multiquark building blocks, has spawned a flurry of research efforts in the Lattice QCD community [10]. The inner workings of QCD and the nature of unstable hadronic resonances, which comprise most of the observed spectrum to

date, will be further illuminated once the grand question of interpretation is resolved. Very few exotic hadrons have been studied on the lattice and thus lack a rigorous theoretical basis.

The class of exotics that we aim to explore are doubly charmed tetraquarks in isospin channels $I = 0, 1$. Namely, the tetraquarks with flavor content $\bar{c}\bar{s}ud$, $c\bar{s}u\bar{d}$, $cc\bar{u}\bar{d}$ and $c\bar{c}u\bar{d}$; The third flavor profile is known as $T_{cc}^{+}(3875)$ [11]. The flavor content is based on the decay channel $D^0D^0\pi^+$ and has isospin 0. The experimental data shows that this is the longest-lived exotic hadron. This exotic has mass of roughly 3875 MeV and manifests as a peak in the mass spectrum of $D^0D^0\pi^+$ mesons. We will use meson-meson interpolators to explore these isospin quantum numbers as opposed to diquark-antidiquark operators; The use of the latter was previously the gold standard in the study of exotic hadrons, but as of late, dimeson operators are primarily used when the heavy quark mass is **not** close to the bottom quark mass. For instance, it is posited that T_{bb} is likely a diquark-antidiquark state, thus, employing diquark-antidiquark operators is important in this case.

The aim of this study is to **establish a pole in the corresponding scattering amplitude $t(E_{cm})$** using distillation smearing on the lattice with coupled dimeson interpolating operators. Assuming we have a suitably large basis of interpolators in the relevant channels of interest, we can compute the spectrum and energy shifts with respect to the DD^* threshold for a heavy quark mass close to the charm quark mass. Moreover, we will investigate whether this species of tetraquark exists within said threshold. We can extract the scattering amplitude from a Lüscher analysis of the lattice data, thereby obtaining the finite volume energies. We endeavor to show that lattice calculations are in agreement with phenomenology, namely, that the DD^* interaction is repulsive in the $I = 1$ channel and attractive in the $I = 0$ channel, which logically follows from the $I = 0$ assignment for the T_{cc}^{+} state.

In Chapter 1 we give a brief background of continuum QCD and the path integral formalism to describe contemporary hadron spectroscopy methods that we employ on the lattice, namely quark field smearing with distillation, and two point correlators. In chapter 2 we describe the computational workflow, tools involved, and the HPC cost associated with the calculation of the eigenbasis, meson elementals, perambulators. Chapter 3 details interpolating operator construction for meson and di-mesons within the distillation framework, the use of derivative (extended) operators, and how to account for mesons at zero and non-zero momentum. The relevant group theory is introduced, to be expanded on in the appendix. In chapter 4 we expand on the end-point analysis of meson correlators and present results for our study of mesonic signal saturation with distillation, specifically the dependence on the size of the distillation basis and number of source insertions. This study dictates the ideal rank of the distillation basis to use when calculating the perambulators and elementals for each ensemble; We can proceed to compute the spectrum and energy shifts with respect to the DD^* threshold for a heavy quark mass close to the charm quark mass. In chapter 5 we describe remaining work, notably a rigorous lattice determination of the quark mass dependence of the $T_{cc}(3875)$ using a large basis of DD^* interpolating operators in various irreducible representations and total momenta. At the end of the day, we must search for poles using finite volume energies from the scattering amplitude, which indicate where an attractive potential is not deep enough to hold a bound state, thus permitting us to make a phenomenological interpretation from the lattice analysis.

CHAPTER 2

Hadron Spectroscopy on the Lattice

2.1 Background

We first provide a brief overview of continuum QCD and how to extract low-energy observables using lattice QCD. In the following section we describe the nature of the so-called signal-to-noise problem which plagues calculations in LQCD, most notably the extraction of hadronic observables. As the Euclidean time between operators increases, the signal-to-noise ratio degrades exponentially. It is standard practice to use quark field smearing algorithms to circumvent this problem and ultimately extract ground-state energies with better statistics. Next, we introduce the method of distillation [12] and the improvements to the signal of correlation functions in contrast to traditional smearing techniques. This will spell out the theoretical basis for the proceeding chapter on operator construction and the computational implementation of described methods to ultimately capture the mesonic and di-meson spectrum, setting the stage for exotic hadrons.

2.2 Continuum QCD

QCD is the gauge theory of strong interactions with color $SU(3)$ as the underlying gauge group. The color degree of freedom was introduced into the quark model to satisfy the Pauli principle. The matter-fields in the theory are quarks (spin-$\frac{1}{2}$) fermions with six flavors and three possible colors (we don't detect these in experiment!). No quark has ever been observed as an asymptotically-free state. During the 1970s, Gell-Mann[6]and others [13][14] tackled the question of exactly which symmetry of the quark model should be gauged. The "hidden" color degree of freedom possessed by quarks is plausible since we only observe color-singlets in nature. Thus, the strong forces between quarks with color need be colorless. Therefore, We can write down the QCD Lagrangian from the free-quark Lagrangian by applying the gauge principle with respect to the color gauge group $SU(3)$. The fundamental objects are the quark fields $q^{(f)}_{\alpha,A}$ where $\alpha : 1,\ldots,4$ are the Dirac-spinor indices, $f : 1,\ldots,6$ denotes the flavor, and $A : 1,2,3$ specifies the color index in the fundamental representation. The QCD Lagrangian is

$$\mathcal{L}_{QCD} = \sum_{f=1}^{6}\sum_{a,b=1}^{3}\sum_{\alpha,\beta,\mu=0}^{3} \bar{q}^{(f)}_{\alpha a}(i(\gamma^{\mu})_{\alpha\beta}(\mathcal{D}_{\mu;ab}) - m_f\delta_{\alpha\beta}\delta_{ab})q^{(f)}_{\beta b} + \sum_{i=1}^{8}\sum_{\mu,\nu=0}^{3} -\frac{1}{4}G^{i}_{\mu\nu}G^{\mu\nu}_{i} \quad (2.1)$$

where $G_{\mu\nu} = \partial_\mu A_\nu - \partial_\nu A_\mu - ig[A_\mu, A_\nu]$ contains the gluons (gauge fields) $A_\mu = \sum_{a=1}^{8} A_\mu^a \lambda^a/2$ where λ^a are the Gell-Mann matrices that index $1, \ldots 8$ corresponding to the adjoint representation of $SU(3)$. The covariant derivative $\mathcal{D}_\mu$ acts on the quark fields like so $\mathcal{D}_\mu q_k = (\partial_\mu - igA_\mu)q_k$ $\mathcal{L}_{QCD}$ exhibits all the symmetries of the quark model and of course all discrete symmetries of the strong interaction, e.g. charge conjugation, parity, and strangeness(since the gluons are flavorless objects) [5]. These symmetries only become manifest via gauge invariance and renormalizability; In fact, $\mathcal{L}_{QCD}$ is derivable from the SU(3) Yang-Mills theory of quarks and gluons, which is devoid of fermions. See [5] for further details on this derivation.

2.2.1 Path integral formulation of QCD

Wilson [15] first introduced lattice gauge theory in 1974 where both space and time are discretized. The quantization of the gauge fields is done via a Wick rotation to Euclidean space $t \longrightarrow i\tau$. We will arrive at this by starting with the real scalar free QFT in Euclidean space,

$$Z_{Eu.}[J] = \int D\phi \exp -\frac{1}{2} \int d^4x \phi^T(x)[\partial^2 + m^2]\phi(x) + \int d^4x J^T(x)\phi(x) \tag{2.2}$$

Now, when we discretize, $\phi(x)$ becomes a column vector

$$\begin{bmatrix} \phi(x_1) \\ \phi(x_2) \\ \cdots \\ \phi(x_n) \end{bmatrix}$$

which manifests as a massive dot product on a computer. $Z_{Eu.}[J]$ becomes $\exp[\frac{1}{2}J^T D^{-1} J]Z[0]$ where

$$Z[0] = \tilde{\phi}(0) = \int d^4x e^{ipx}\phi(x) \tag{2.3}$$

In order to compute correlation functions, we need functional derivatives:

$$\frac{\partial}{\partial J_y}\frac{\partial}{\partial J_x} Z[J]|_{J=0} = D^{-1} = \langle 0|\hat{\phi}(y)\hat{\phi}(x)|0\rangle \tag{2.4}$$

where the matrix element is again a time ordered product. In momentum space, the partition function is

$$Z_{Eu.}[J] = \int \underbrace{D\tilde{\phi}_p}_{\prod_{p_i} d\phi_{p_i}} \exp[-\tfrac{1}{2}\textstyle\int_x \int_p \int_{p'} \tilde{\phi}^T(p)[p^T + m^2]\tilde{\phi}(p) e^{i(p-p')x}] \tag{2.5}$$

$$= \textstyle\int \prod_{p_i} d\phi_{p_i} \exp[-\frac{1}{2}\tilde{\phi}^T(p_i) D_{p_i} \tilde{\phi}_{p_i}] \tag{2.6}$$

Using properties of Gaussian integrals,

$$Z[0] = N\frac{1}{\sqrt{\det(D)}} \tag{2.7}$$

with the Fermionic piece

$$\det(D)e^{J^T D^{-1} J} \tag{2.8}$$

Wilson's formulation of the Feynman path integral of QCD as a statistical mechanical sampling of the related Euclidean spacetime integral path

$$Z_{QCD} = \int DA_\mu D\psi D\bar{\psi} \quad \exp\left[-\int \bar{\psi} D[A_\mu]\psi - \frac{1}{4}\underbrace{G^2}_{\text{Gauge field Lagrangian}}\right] \tag{2.9}$$

We have to compute the Grassman numbers by hand

$$Z_{QCD} = \int DA_\mu \det D[A_\mu] e^{\underbrace{\frac{-1}{4}G^2}_{\text{Gauge action}}} \tag{2.10}$$

Which implies that for every configuration of "Glue"(gauge fields), we have to know the value of the determinant. As we shall see, we don't actually evaluate this determinant, rather, we introduce "pseudo-fermions" into the QCD partition function

$$Z_{QCD} = \int DA_\mu D\phi^* D\phi e^{\left(\frac{-1}{4}G^2 - \phi^{*T} D^{-1}_{A_\mu}\phi\right)} \tag{2.11}$$

where $D^{-1}_{A\mu}$ is a large sparse matrix with small eigenvalues. Now we have

$$\text{(Exactly solvable Gaussian)} \times \int d\phi d\phi^* e^{-\phi^* T D^{-1}\phi} \tag{2.12}$$

$$= \left(\frac{1}{\det(D)}\right)^{-1} \tag{2.13}$$

$$= \det(D) \tag{2.14}$$

which illuminates the large computational cost required of sparse matrix inversions, luckily, modern GPUs handle matrix multiplication well. Define an example Lattice universe of size $32^3 \times 96$ where $N_x = N_y = N_z = 32, \quad N_t = 96$. Express 4D spacetime as a column vector:

$$\underbrace{\psi(x)}_{field} = 32^3 \times 96 \times \underbrace{3}_{color} \times \underbrace{4}_{spin} = 12 \times 3145728 \quad \text{sites} \tag{2.15}$$

The modus operandi is thus to manipulate matrices of this size with the computer. As a brief foray

into the computational considerations, which will be further hashed out in the next chapter, consider the compute time of a matrix inversion:

$$t_{cpu}\left(D^{-1} = \frac{\lambda_{max}}{\lambda_{min}}\right) \quad \text{(eigenvalues)} \tag{2.16}$$

$$\lambda_{QCD}[D] \sim m_{u,d} \qquad ; \quad m_{u,d} \ll \Lambda_{QCD} \ll \frac{1}{a} \tag{2.17}$$

$$t_{cpu}[\text{volume}] \approx \left(\frac{L}{a}\right)^4 \frac{1}{am_q} \underbrace{\frac{1}{a}}_{\text{discretization penalty}} \sim \frac{1}{a^6} \tag{2.18}$$

So we can deduce the scaling

$$a \to \frac{1}{2}a \equiv 64 \times \text{orig}(t_{\text{cpu}}) \tag{2.19}$$

where the coarse graining of the lattice spacing a is necessary in order to recover the continuum theory. With this formulation in hand, we can explicitly form the lattice gauge theory. Let

$$S = \int d^4x \mathcal{L}(x) \tag{2.20}$$

$$S_{LQCD} = \sum_{nm} a^{n-4} \alpha_s^m S_{n,m} \tag{2.21}$$

where $n \geq 4, m \geq 0$. This is an expansion about the continuum limit, the first term in the expansion is exactly QCD. The remaining terms are the discretization effects resulting from the theory being transcribed in a finite box with boundary conditions. If we extrapolate to 0, we exactly recover the continuum theory of QCD. It needs to be emphasized that LQCD is indeed the only non-perturbative regularization scheme in the infrared regime that is systematically improvable, meaning one can dial the input parameters. This improvement manifests itself via the following properties of discretized spacetime, which are tightly coupled to high-performance computing architecture. The crucial feature of this discretized version of the continuum theory is gauge covariance, namely $m_{gluon} \to 0$, which is the only way the theory can remain renormalizable without adding new terms.

- Discretization scale (a) where there are no infinities at finite values of a
- Finite Volume
- Unphysical quark mass, which allows us to extrapolate to the physical quark mass with effective field theory

Discretization of a continuum theory naturally lends itself well to being transcribed onto a computer. In essence, we perform LQCD calculations on some HPC cluster, encode known properties of QCD into some EFT (e.g. Chiral perturbation theory, Baryon χPT, etc. which will not be discussed in this work) to make predictions about the standard model. The tunable parameters of LQCD simulations are the coupling constant α_s and the quark masses modulo the top quark. Modern computing power allows us to perform these at the physical pion mass.

2.2.2 Discretization of the Fermion and Gauge Actions

Wilson's goal was to quantize a gauge field theory on a discrete lattice in Euclidean space-time while preserving exact gauge invariance [15]. The expansion about the strong coupling constant requires summing over all possible quark paths and all surfaces that join these paths.

Using results from general field theory, we can write down the following relation

$$\langle 0|T\hat{\phi}_N(x_N)\dots\hat{\phi}_1(x_1)|0\rangle \equiv \frac{1}{Z}\int D\phi\phi(x_N)\phi_1(x_1)e^{i\int d^4x\mathcal{L}(\phi,\partial\phi)} \tag{2.22}$$

We can write down the partition function $Z = \int D\phi e^{iS}$. The former is a time ordered-product of fields, which is hard to put on a computer but allows us to predict what we should see. The latter is composed of commuting numbers and an infinite dimensional integral over all gauge configurations, which we cannot naively calculate on a computer. However, we know that a computer, with suitable hardware architecture, can handle all IR non-pertrubative physics.

We first need to discretize the hypercube into a grid with volume N^4 = number of sites where N is the spatial extent. Next, we perform a Wick rotation $t \to -i\tau$ to Euclidean spacetime so that the partition function becomes

$$Z_{Eu.} = \int D\phi_{Eu.} \quad \underbrace{e^{(-SE_u)}}_{\text{Probability weight}} \tag{2.23}$$

In order to find the most "valuable" configuration on our lattice, we must run a Monte Carlo simulation. This must satisfy the Ergodic hypothesis; The simulation must be able to run in both directions in Monte Carlo time. Now we can generate an ensemble of ϕ^i's

$$\phi^i_{Eu.} : i - 1, \dots N \tag{2.24}$$

that minimize the Euclidean action $S_{Eu.}$. Said another way, these are the trajectories that are as close to the classical action as possible; This is akin to how one can recover classical mechanics from quantum mechanics.

2.3 Wilson's Lattice Quantization of Gauge Fields

In this section we capture how Wilson defined the space-time integral of the QCD Lagrangian on a discrete lattice in Euclidean space-time. Put simply, the derivatives present in the continuum action are substituted with finite-differences and the integral over space-time is replaced with a sum over lattice sites. The action must be gauge invariant for any lattice spacing a. Fermion fields live at every lattice site n $\phi(x) \to \phi_n$; We connect these fermions with oriented link variables (direction matters!) in order to retain gauge invariance.

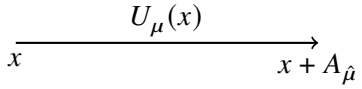

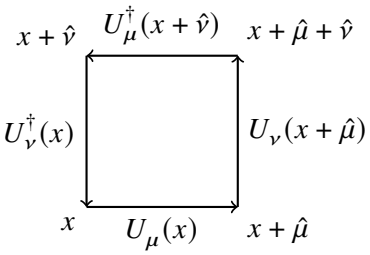

The fundamental square of a hypercubic lattice is the plaquette, $U_{\mu\nu}(x)$ is an oriented square. The trace of $U_{\mu\nu}(x)$ is a gauge-invariant object, thereby allowing the gauge-field piece of the action in lattice units

$$U_{\mu\nu}(x) = \mathrm{Tr}\left[U_\mu(x)U_\nu(x+\hat{\mu})U_\mu^\dagger(x+\hat{\nu})U_\nu^\dagger(x)\right] \tag{2.25}$$

The Wilson gauge action, simple and unimproved, is a sum over all plaquettes

$$S_G[U] = \frac{2}{g^2}\sum_{n\in\Lambda}\sum_{\mu<\nu} Re\left(Tr\left[\mathbb{I} - U_{\mu\nu}(x)\right]\right) \tag{2.26}$$

where the coefficient is the inverse gauge coupling. In Euclidean space, this becomes

$$S_G[A] = \frac{1}{2g^2}\int d^4x Tr\left[F_{\mu\nu}(x)F_{\mu\nu}(x)\right] \tag{2.27}$$

We take the trace over color indices because the gluon fields are matrix valued, which keeps the action invariant under gauge transformation. To recapitulate, we have the following now at our disposal:

- $U_\mu(x)$ is a link variable connecting sites $x, x+\mu$
- Gauge transformation $U_\mu(x) \to U'_\mu(x) = \Omega(x)U_\mu(x)\Omega(x+\hat{\mu})^\dagger$

Where the gauge fields $U_\mu(x)$ and $\Omega(x)$ are both elements of $SU(3)$ on each lattice site. We want to define a lattice gauge transporter with these attributes. In the continuum, a candidate that possess such properties would be a path-ordered exponential integral of the gauge field A_μ along some curve C_{xy} that connects the points x, y

$$G(x,y) = p\cdot\exp\left(ia\int_{C_{xy}} A_\mu(x)\cdot ds\right) \tag{2.28}$$

, so we need a link variable $U_\mu(x) = G(x,y) + \sigma(a)$ where $\sigma(a)$ are the higher order corrections. Wilson's choice was

$$U_\mu(x) = \exp\left(iaA_\mu(x)\right) \tag{2.29}$$

Therefore, by defining a link variable, we restore the gauge invariance. If we did not, then the gluon would be massive. Now we can write down what is called the *Symanzik Expansion*

$$\lim_{a\to 0} S_{LQCD} = S_{QCD} + \underbrace{aS^5_{LQCD} + a^2S^6_{LQCD}}_{\text{discretization corrections}} \tag{2.30}$$

where the lattice spacing $a = \frac{1}{\Lambda_{\mu\nu}}$. We can systematically control the above discretization errors by generating ensembles with various lattice spacings.

This formulation begs the question; We have been working in Euclidean space, why can we not just use Minkowski space? The action in Minkowski is a wildly oscillating integral

$$Z_\mu = \int DA_\mu \det\left[D[A_\mu]\right] e^{i\sum_x \frac{1}{4} G_{\mu\nu}G^{\mu\nu}} \tag{2.31}$$

with no known algorithm to solve it. However, back in Euclidean space, we have

$$Z_{EU} = \int DA_\mu \det\left[D[A_\mu]\right] e^{-\sum_x \frac{1}{4} G^{EU}_{\mu\nu}G^{EU}_{\mu\nu}} \tag{2.32}$$

where the term in exponentiated sum is S_G or S − "glue". $e^{-S_G} \in \mathbb{R}$ so we can use Monte Carlo probability sampling to determine which G's are important, namely those which minimize the classical action. Moreover, we don't want to wick rotate back to Minkowski space $-i\tau \to t$, all physics can be extracted from Euclidean space. The hadron spectrum can be easily computed, but we cannot compute scattering processes directly in Euclidean space (this is where the Lüscher Quantization condition enters).

Finally, we take Wilson's choice $U_\mu(x) = \exp\left(iaA_\mu(x)\right)$ and insert it into the expression for the plaquette $U_{\mu\nu}(x)$ and apply the Baker-Campbell-Hausdorff theorem[16] to obtain the expression for the plaquette

$$U_\mu\nu(x) = \exp\left(ia^2 F_{\mu\nu}(x) + O(a^3)\right) \tag{2.33}$$

where $F_{\mu\nu}(x) = -i\left[D_\mu(x), D_\nu(x)\right]$ is a commutator of covariant derivatives.

The general form of the **Lattice version of the fermion action** is

$$S_F^0 = a^4 \sum_{x\in\Lambda} \bar{\psi}(x)\left(\sum_{\mu=1}^{4} \gamma_\mu \frac{\psi(x+\hat{\mu}) - \psi(x-\hat{\mu})}{2a} + m\psi(x)\right) \tag{2.34}$$

and the general form **Lattice version of the Gluon action is**

$$\frac{2N_c}{g^2} \sum_x \sum_{\mu<\nu} \left(1 - Re(Tr(U_\mu\nu(x)))\right) \tag{2.35}$$

where $U_\mu\nu(x)$ can be freely substituted with a different plaquette. It is legal to add terms to the discretized actions, as is done in the Symanzik improved gluon action that we employ, so long as the additional terms vanish in the continuum limit.

In summary, $S_{\text{LQCD}} = S_G + S_F$, which must be dimensionless.

$$\langle 0|\sigma_{\text{QCD}}|0\rangle_{\text{QCD}} = \lim_{\substack{a\to 0 \\ m_q\to\text{phys} \\ N\to\infty \\ V\to\infty}} \langle 0|\sigma_{\text{LQCD}}|0\rangle_{\text{LQCD}} \tag{2.36}$$

Which substantiates the statement that QCD is defined as LQCD as the lattice spacing goes to 0; With infinite compute time we can exactly solve QCD under one assumption, which is that we are

in the right phase of the theory. Well, we cannot take $a \to 0$ as we are bound by classical compute architecture and finite time. However, we can let the lattice spacing $a \gg$ any interesting scale in QCD which implies the relation $\frac{1}{a} \gg \Lambda_{QCD}$.

2.4 Two-Point Euclidean Correlation Functions

A correlator of two Hilbert-space operators $\phi, \phi^\dagger$ is written as

$$\langle 0|T\{\phi(y)\phi^\dagger(x)\}|0\rangle \tag{2.37}$$

and we can insert a complete set of states $1 = \sum_n |n \times n|$.

$$\sum_n \langle 0|e^{Hy_0}\phi(0,\vec{y})e^{-Hy_n}|n \times n|e^{Hx_0}\phi^\dagger(0,\vec{x})e^{-Hx_n}|0\rangle \tag{2.38}$$

At definite momentum,

$$C(\tau,\vec{p}_f,x) = \sum_n \underbrace{\sum_y e^{i\vec{p}_f\vec{y}} Z_{yn}}_{Z_{n\vec{p}}} Z^\dagger_{xn} \exp\left(-E_n \underbrace{(y_0 - x_0)}_{-it\to\tau}\right) \tag{2.39}$$

It is worth noting that both the Fourier transform of x, y need not be computed; If you performed both, this results in N_L^3 additional computational cost. At zero momentum,

$$C(\tau,\vec{p}_f = 0,x) = \sum_n Z_{n0}Z^\dagger_{nx}e^{-m_n\tau} \tag{2.40}$$

We can pick off the spectrum by taking the long-time limit:

$$\lim_{\tau\to\infty} C(\tau,\vec{0},x) = Z_{0\vec{x}}Z^\dagger_{0\vec{x}}Z_{n\vec{p}} \tag{2.41}$$

$$Z_{n\vec{p}} = \sum_{\vec{y}} e^{i\vec{p}\vec{y}} \langle 0|\phi(0,\vec{y})|n\rangle \tag{2.42}$$

$$\lim_{\tau\to\infty} C(\tau,\vec{0},x) = Z_{0\vec{x}}Z^\dagger_{0\vec{x}}Z_{n\vec{p}}e^{-m_0\tau}(1 + \delta Z_{10}\delta Z^\dagger_{1x}e^{-\delta m_{10}\tau} + \ldots \text{H.O.C}) \tag{2.43}$$

$$\tag{2.44}$$

Now the correlator can be fit with a decaying exponential using Bayesian methods to extract the ground state energy and the variational method to extract excited state properties which use multi-exponential fit functions.

$$C_{ij}(\tau,\vec{p},\vec{x}) = \sum_{\vec{n}} e^{-E_n\tau} Z^{(i)}_{n\vec{p}} Z^{\dagger(j)}_{n\vec{x}} \tag{2.45}$$

We will present the distilled meson correlator for an isovector meson in Chapter 4.

2.4.1 Summary of LQCD Formalism

In a nutshell, we have

- Replaced continuous spacetime by a 4D Euclidean lattice with a constant lattice spacing a. The DOF are classical field variables ϕ living on the lattice.
- Construct the Euclidean action $S_{EU}[\phi]$ of the discretized system such that $\lim_{a\to 0}$ of the Euclidean continuum action is obtained with the Boltzmann factor weight $e^{-S_{EU}[\phi]}$
- Operators in the Euclidean correlator of interest translate to functional by replacing field operators with classical lattice field variables
- Compute Euclidean correlation functions by evaluating these functionals on some lattice gauge field configuration weighted with the Boltzmann factor and integrated over all possible field configurations.

2.5 Gauge Field Smearing

Gauge links, the edges on the lattice connecting the vertices(quark sites), are the discretized version of gluons in the continuum theory of QCD. They are known to introduce noise in the form of short range fluctuations. To circumvent this, different types of "smearing" are typically applied during the generation of ensembles. In order to achieve overlap with states of interest in the continuum, namely the low-lying eigenstates, one must being with smearing of the quark fields via some smoothing function. A brief exposition of *Jacobi smearing* will follow to motivate our implementation of *distillation smearing*.

It is advantageous in LQCD calculations to first "smear out" the high-energy modes from the fermion fields at each time-slice. This will make the extraction of the energy spectra realizable at earlier times, since if the high-energy modes were still present, the asymptotic behavior of the correlator would not manifest until much later. Both the link variables(gluons) $\tilde{U}_j(x)$ and quark fields $\tilde{\psi}(x)$ are spatially-smoothed. The temporal link variables are not smoothed. For each quark flavor, the quark field is smoothed with the operator

$$\tilde{\psi}_{a\alpha}(x) = \mathcal{S}_{ab}(x,y)\psi_{b\alpha}(y) \tag{2.46}$$

Here, x, y are lattice sites, a, b are color indices, α a spin component.

$$\tilde{\Psi}(\vec{x},t) = \sum_{\vec{y}} L(\vec{x},\vec{y})\psi(\vec{y},t) \tag{2.47}$$

The simplest smearing operator is a gauge-covariant Laplacian, called the Jacobi operator [12]

$$J_{\sigma,n_\sigma}(t) = \left(1 + \frac{\sigma\nabla^2(t)}{n_\sigma}\right)^{n_\sigma} \tag{2.48}$$

where ∇^2 is [1]

$$\nabla^2(a,b;t) = -6\delta_{a,b} + \sum_{k=1}^{3}\left(U_k(a,t)\delta_{a+\hat{k},b} + U_k^\dagger(a,t)\delta_{a-\hat{k},b}\right) \tag{2.49}$$

where σ is a free parameter. By using this smearing operator, we can perform all-to-all quark propagation measurements. This construction is called distillation, which we will revisit in the next section. We employ 6-stout smearing [17] and add smear the quark fields using distillation in the proceeding phase of the computational chain [12]. Here we briefly describe stout smearing and arrive at the definition of a stout link.

2.5.1 Stout Smearing

Each gauge link on the lattice has four neighboring staples. Let $C_\mu(x)$ denote the weighted sum of the perpendicular staples which begin at lattice site x and terminate at neighboring site $x+\hat{\mu}$, this formulation was introduced by [17]:

$$\begin{aligned} C_\mu(x) &= \sum_{\nu\neq\mu}\rho_{\mu\nu}\Big(U_\nu(x)U_\mu(x+\hat{\nu})U_\nu^\dagger(x+\hat{\mu}) \\ &\quad + U_\nu^\dagger(x-\hat{\nu})U_\mu(x-\hat{\nu})U_\nu(x-\hat{\nu}+\hat{\mu})\Big), \end{aligned} \tag{2.50}$$

This is the formulation of a plaquette, where the magnitude of the vectors $\hat{\mu}, \hat{\nu}$ is the length of a single lattice spacing (given by the particular ensemble) and the weights $\rho_{\mu\nu}$ are tunable.

2.6 Distillation Smearing

The computation of all-to-all quark propagators is crucial in LQCD calculations of correlation functions for a suitably large set of interpolators. This is computationally expensive as the number of "solves" of the lattice Dirac matrix scales with the spatial and temporal extent of the lattice. By projecting quark fields into a subspace with rank less than that of the original vector space of fields on a time-slice, we can reliably compute all-to-all propagators[12]. Within this reduced subspace, we can project operators onto definite momentum at both the source and sink. Hermiticity of operators is also guaranteed with this method, which bodes well for solving the GEVP within each irrep of interest. As scattering studies require well-controlled momentum insertions, this will serve us well at later stages of the T_{cc}^+ analysis. The first order of business it to solve for the first N_D eigenvectors with the smallest eigenvalues of the gauge-covariant Laplacian such that

$$-\nabla^2 V = VD \tag{2.51}$$

The information we need to extract is

$$V^\dagger M^{-1} V \to \tau$$

where τ is the perambulator matrix on a single time slice. $V(t)$ is a matrix with $4 \times N_v$ columns constructed from eigenvectors of the covariant 3d Laplace operator. It is important to note that $V(t)$ does not act on Dirac components. Thus, $V(t)$ is a block identity in Dirac space and each block contains the first N_v eigenvectors $v_i(t)$. A given column $V^{(i,\alpha)}(t)$ has entries

$$V^{(i,\alpha)}(t)_{\vec{x},t',\beta} = v_i(t)_{\vec{x}}\delta_{tt'}\delta_{\alpha\beta}$$

Propagators transform with tensor product structure

$$\text{Lattice} \otimes \text{Matrix(Nc)} \otimes \text{Matrix(Ns)} \otimes \text{Complex}$$

We can work out these dimensions for ourselves; A distilled propagator stored on disk has dimensions

$$2 * 8 * 2 * 4 * 4 * 10 * 10 * 16 \tag{2.52}$$

with the dictionary

$$\text{complex} * \text{snk} * \text{src} * N \times N_\sigma * \text{tslice} \tag{2.53}$$

In the next section covering the computational aspects of this project, we will delve slightly deeper into how this is accomplished with HPC and the `Chroma` software stack.

2.7 Contractions

At this point, we need to actually perform contractions to obtain the correlator. This is a sum over all the spin and color perambulator indices with spin matrices and color tensors, thus creating colorless objects satisfying the gauge invariance of QCD. We analyze the Monte Carlo ensembles of correlation functions on a configuration by configuration basis.

$$O = \sum_{i,j} A_{ij}[(\bar{u}\Gamma_i c)(p_i^1)(\bar{d}\Gamma_j c)(p_i^2) - (\bar{d}\Gamma_i c)(p_i^1)(\bar{u}\Gamma_j c)(p_i^2)],$$

where $\Gamma_{i/j}$ represents the appropriate Dirac structure and the momenta p^1 and p^2 add up to zero, as we will stay in the rest frame within this period.

$$C_M^{(2)}(t',t) = Tr[\Phi^B(t')\tau(t',t)\Phi^A(t)\tau(t,t')]$$

where

$$\Phi^A_{\alpha\beta}(t) = V^\dagger(t)[\Gamma^A(t)]_{\alpha\beta}V(t) \equiv V^\dagger(t)\mathcal{D}^A(t)V(t)S^A_{\alpha\beta}$$

is the elemental building block and

$$\tau_{\alpha\beta}(t',t) = V^\dagger(t')M^{-1}_{\alpha\beta}(t',t)V(t)$$

is the perambulator, defined by the lattice representation of the Dirac operator, M. This defines the distilled "version" of a quark propagator connected distillation spaces on two time slices t, t'.

CHAPTER 3

Computational Considerations

The amount of compute time for generating the eigenbasis, and subsequently the perambulators and meson elementals, scales with the spatial extent of the lattice N and the rank of the distillation basis n. We provide an overview of our lattice setup and a summary of the Hybrid Monte Carlo method for generating gauge configurations. Next, we present the software stack and pipeline for our calculations on the Jureca cluster, including the storage and runtime cost associated with each object necessary for performing hadron spectroscopy with distillation. As this framework hinges upon algebraic mulitigrid methods, we touch on the key points and how this technology interfaces with `Chroma` lattice objects. At the final stage, matrix elements(meson elementals) and perambulators are contracted together with some appropiate Dirac strucutre depending on the flavor and isospin channel (the J^{PC} continuum quantum numbers to be accessed), which we elucidate diagramatically. The details of our 6-stout smeared ensembles are given for completion. Having a wide range of pion masses and lattice spacings to study will allow us to probe the quark mass dependence of the exotic doubly charmed tetraquark state T_{cc}^{+}.

3.1 Lattice Setup

The only known *ab-initio* approach to probing the low energy regime of QCD is with High Performance Computing(HPC) and the discretized lattice. At bottom, a path-integral approach is used to compute some observable O with a predefined collection of bare physics and lattice parameters$\{\beta, am_{ud}, am_{s}\}$. Again, the lattice path integral is:

$$Z = \int [DU] \exp\left[-S[U]\right] \quad \text{where} \quad DU = \prod_{x,\mu} dU_{\mu x} \tag{3.1}$$

where one can add in the dependence on the bare physics and lattice parameters like so:

$$\langle | \, O \, | \rangle = \frac{1}{Z} \int \mathcal{D}[U] O(U) \cdot p(U) \tag{3.2}$$

where $p(U)$ is built from the discretized Dirac operator and pure gauge action and the integral measure is $\mathcal{D}[U] = \prod_{x=0,\mu=1}^{d,V} dH(U_{\mu}(x))$ where V is the volume of the lattice in $d = 4$ dimensions (the lattice

is a hypercube, a 4D object) and the Haar measure dH, which allows the lattice path integral to retain gauge invariance. The data in this problem spaces is contained in the lattice sites.

In we showed how the discretization of the euclidean path integral reduces the infinite number of integrals to something more manageable. However, the number of lattice sites on a typical lattice is $\approx 32^4$, so a "brute-force" approach is not feasible. See [18], [19],[20] [21] for more details. To make the problem tractable, we turn to Markov Chain Monte Carlo simulations to calculate the expectation value and correlation functions of observables

$$\langle O \rangle = \frac{1}{N} \sum_{q,\bar{q},U} O\left[q, \bar{q}, U\right] \tag{3.3}$$

where $[q, \bar{q}, U] \approx \exp(-S[q, \bar{q}, U])$. The latter is the probability weight that we use to perform importance sampling of the gauge field configurations. This is necessary because only a small vicinity of the minimum of the spectral density will contribute. Moreover, The Boltzmann factor $\exp(-S[\phi])$ dictates the distribution of configurations in the sample produced by the Monte Carlo integration. This process is comprised of two steps [19]:

- Proposal: a new gauge configuration U' is generated with some weight $q(U)$ with probability $T(U \to U')$
- Correction or Updating: $P_{accept}(U, U') = \min\left[1, \frac{p(U')q(U)}{p(U)q(U')}\right]$

Assuming that the above ratio follows a log-normal distribution then the acceptance rate is $\texttt{erfc}\left(\sqrt{\sigma^2/8}\right)$ where erfc is the complementary error function. The collection of configurations U_i with associated weight $p(U)$ make up the ensemble.

3.2 Software Stack for Distillation

Distillation is costly initially both in storage and component construction. This pays off at the end of the day as we can reuse the perambulators for subsequent calculations; The inversions can be precomputed and stored on disk. For the di-meson system we are investigating, the contraction cost is not the dominant contribution. We will use the MultiGrid (MG) solver from `QUDA`, `Chroma` with `Superbblas` support, the `PRIMME` eigensolver, and `Numpy Einsum` for contractions. The amount of computation and storage scales with the lattice size N and the rank of the distillation basis, n. The optimal rank of the distillation basis is determined experimentally, but it is proportional to the spatial volume of the lattice. All of the high-peformance computing tasks below were performed on the Jureca cluster at the Juelich Supercomputing Centre.

3.3 Pipeline

In order to perform spectroscopy calculations for a given ensemble, there exists a sequential dependency chain for HPC calculations:

✓ **Ensemble generation:** $N_f = 2 + 1$ quark flavors, a tree level Symanzik improved gluon action and 6-stout dynamical smeared Wilson fermions

✓ **HPC Tasks:** Generation of distillation basis, perambulators, meson elementals using `Chroma` with `superbblas` support on the Jureca cluster at JSC

- Construct **Di-meson distilled operators** using Hadspec method of subduction coefficents and helicity operators

✓ Perform **contractions** of multi-hadron operators → 2pt correlators

- Construct correlation function coming from the **GEVP** in the right irreducible representation

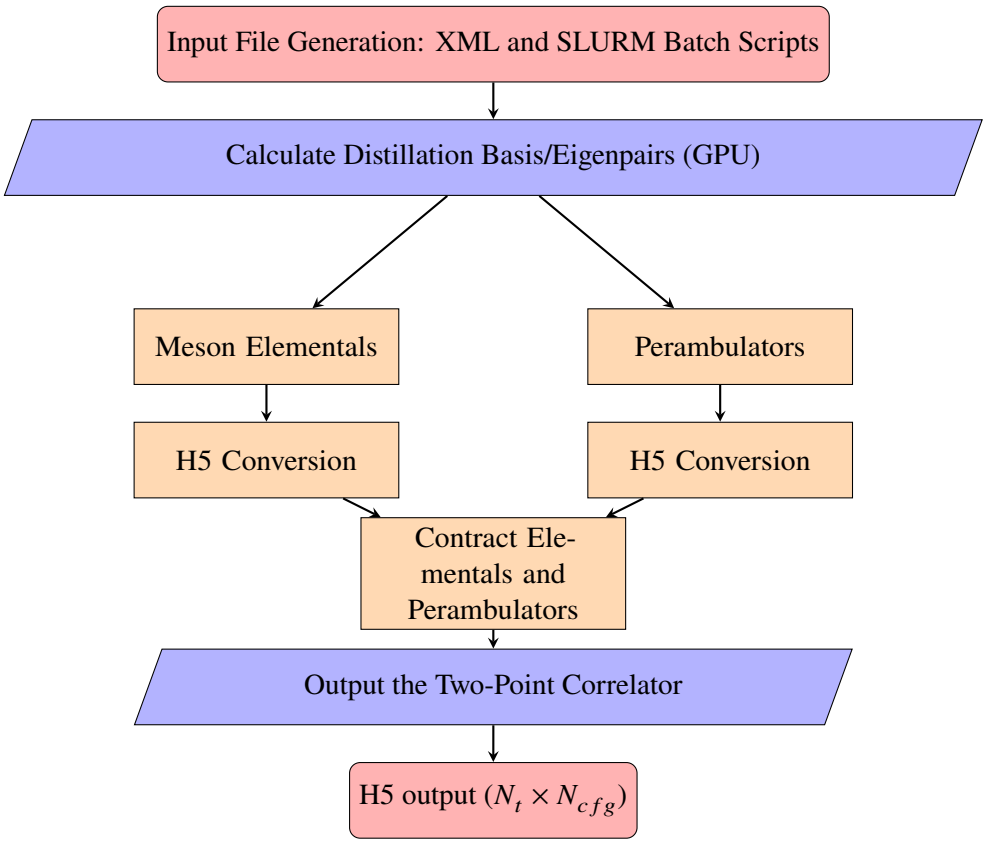

Figure 3.1: Flowchart of the computational workflow for computing lattice objects with distillation.

3.4 Multigrid Methods in LQCD

Computing fundamental building blocks on the lattice, which will each be discussed in the proceeding sections, requires sophisticated hardware architecure. We use the `Chroma` software stack from USQCD [22] compiled with `superbblas` support (required for computing the distilled objects of interest), and the multigrid solver from `QUDA`. We run the HPC tasks on a single GPU node, as we found multi-node

	Lattice		*Color*		*Spin*		*Complexity*
Gauge fields :	Lattice	⊗	Matrix(Nc)	⊗	Scalar	⊗	Complex
Fermions :	Lattice	⊗	Vector(Nc)	⊗	Vector(Ns)	⊗	Complex
Scalars :	Scalar	⊗	Scalar	⊗	Scalar	⊗	Scalar
Propagators :	Lattice	⊗	Matrix(Nc)	⊗	Matrix(Ns)	⊗	Complex
Gamma :	Scalar	⊗	Scalar	⊗	Matrix(Ns)	⊗	Complex

Table 3.1: The tensor structure of `Chroma` objects. `Nd`: num. space-time dimensions, `Nc`: dimension of the color vector space, `Ns`: dimension of the spin vector space. [22]

jobs are not compatible with our stack and the Jureca cluster at JSC. This stack ultimately allows us to calculate a large class of matrix elements at high precision [23] using distillation.

Before we dive into the details of the calculation of our distilled objects, it is useful to show how lattice objects in `Chroma` transform under different spaces with a tensor product structre [22]. Gauge fields can left-multiply fermions via color matrix × color vector but is diagonal in spin space (spin scalar × spin vector). A Γ matrix can right-multiply a propagator (spin matrix × spin matrix) but is diagonal in color space (color matrix × color scalar). Say we have two lattice fermion fields A, B, a lattice color matrix, or gauge field `U`. At each lattice site, `U` is a scalar in spin space. The product

$$B^i_\alpha(x) = U^{ij}(x) \times A^j_\alpha(x) \tag{3.4}$$

for lattice coordinates x, i, j are the color indices, and α is the spin index. The tensor multiiplication is over complex types, from which we will extract the real component at the stage of forming two point hadron correlators.

3.4.1 Eigenpairs/Distillation Basis Calculation

Sparse linear algebra is necessary to construct the smeared quark fields based on distillation, where the eigenvectors with smallest eigenvalues of the gauge-covariant Laplace operator $\nabla^2[t]$. This is the first step in the calculation which is input data for the generation of elementals and perambulators. We use the `Primme` eigensolver to obtain the eigenpairs(eigenvalues,eigenvectors) of the Hermitian Wilson-Dirac operator[24][25]. The eigenbasis in distillation space contains the eigenvectors from the lowest-lying regime of the spectrum of the hermitian negative-definite Laplacian-like operator

$$\nabla^{2(\vec{x},\vec{y})} = 6\delta_{\vec{x},\vec{y}} - \sum_{\vec{j}\in|(1,0,0),(0,10),(0,0,1)|} U^{(x)}_{\vec{j}}\delta_{\vec{x}+\vec{j},\vec{y}} + U^{(\vec{x}-\vec{j})^\dagger}_{\vec{j}}\delta_{\vec{x}-\vec{j},\vec{y}} \tag{3.5}$$

where the gauge fields U are stout smeared. Distillation smearing projects into the N_D dimensional vector space like so

$$\Box_{ab}(x_1, x_2, t) = V(x_1, t)^d_a V^\dagger(x_2, t)^d_b \tag{3.6}$$

where a, b are the color indices and $d = 1 \ldots N_D$ is the distillation space index [1]. This is the eigenbasis in distillation space, which now allows us to access elements of the quark propagator.

3.4.2 Calculating Meson Elementals

The calculation of our elemental building blocks requires tensor contractions. These matrix-matrix multiplications are accelerated with the `Superbblas` library [26]. These objects are calculated for every time-slice, on every gauge configuration, and with every combination of displacements. If we disregard the perambulators for a moment, the correlation functions are described by the correlation between meson elementals at the different time-slices. We can write the distilled meson elemental as

$$\Phi^A_{\alpha\beta}(t) = V^\dagger(t)[\Gamma^A(t)]_{\alpha\beta}V(t) \equiv V^\dagger(t)\mathcal{D}^A(t)V(t)S^A_{\alpha\beta} \tag{3.7}$$

where $\mathcal{D}^A(t)$ is the lattice Dirac matrix and $S^A_{\alpha\beta}$ is the subduction coefficient, which is the identity for $\vec{P}^2 = 0$. For non-zero displacement, the Γ operator is no longer trivial in position and color space and requires single or double covariant derivatives, ∇_i where i is in the x,y,or z direction, to act on the 3D spinor components at some time t. In the later section on derivative operators, we will show how this is expressed in the language of `Chroma`. For completeness, the elemental form for zero, single, and double derivative displacement, respectively, are:

$$V^\dagger(t)[\Gamma^A(t)]_{\alpha\beta}V(t) \tag{3.8}$$

$$V^\dagger(t)[\nabla_k(t)]_{\alpha\beta}V(t) \tag{3.9}$$

$$V^\dagger(t)[\nabla_k(t)\nabla_l(t)]_{\alpha\beta}V(t) \tag{3.10}$$

This tensor contraction involves the following[23]:

- Two 5-dimensional tensors (the distillation basis) v, w, the coordinates of which are on the **spatial** extent of the lattice N_L, three color space components, and the distillation basis column index
- 4-dimensional tensor z representing a phase $z^{\vec{x},l} = e^{-i\vec{p}\vec{x}}$ which carries a component in N_L as well as a momentum index
- color contraction with the projector into color space, the Kronecker delta, where $\vec{x} \in N_t, \alpha, \beta \in C$

  $M^{i,j,l} = \sum_{\vec{x},\alpha,\beta} \delta^{\alpha\beta} v^{\vec{x},\alpha,i} w^{\vec{x},\beta,j} z^{\vec{x},l}$ for $1 \le i, j \le n, 1 \le l \le M$

which is performed at different time slices in parallel.

3.4.3 Calculating Perambulators

The perambulator characterizes the distilled version of a quark propagator from time t_0 to some later time t_f and all combinations therein for the entire temporal extent N_t of the lattice [12]

$$\tau[t_0, t_f]^{\alpha\beta}_{ij} = v_{i,\alpha}[t_0]^\dagger D^{-1} v_{j,\beta}[t_f] \tag{3.11}$$

where we can factorize these $4N_v \times 4N_v$ matrices like so

$$(4 \times 4) \otimes (N_v \times N_v) \tag{3.12}$$

yielding $16N_v^2$ inner products and $4N_v$ inversions. One can immediately form the perambulator $\tau(t_0, t_f)$ for all values of t_0 after solving for the vector $D^{-1}v_{j\beta}[t_f]$ on each configuration; Each configuration will have its own perambulator binary file containing information over all possible time slices. We use the Wilson-Clover multigrid solver from `QUDA` [27] specifically the GCR solver(a Krylov solver) to calculate the linear system of equations

$$Dx^{i\alpha} = v_{i\alpha}(t) \tag{3.13}$$

where i is the rank of the distillation basis, α is a color index, and t is indexed along the temporal extent of the lattice.

3.5 Cost and Storage of Distillation

As we highlighted in the previous section, distillation restricts operators to a small subspace while maintaining overlap with relevant eigenstates. As the computational cost is directly proportional to the size of matrices one is manipulating, a reduction in the rank of operators slashes the cost of computing the propagation matrix. Once a suitable set of perambulators are computed, we can reuse them to correlate a collection of interpolators.

Computation	Operations cost	Memory footprint
Distillation basis[a]	N^3Tn^3	N^3nT
Meson elementals[b]	N^3Tn^3	$N^3n + n^3$
Perambulators[c]	N^3Tn	N^3Tn
Contractions[d]	n^4T	n^3T

[a] Generate colorvector matrix elements
[b] Contract two matrices → tensor
[c] Projection of the inverse Dirac operator → square matrices
[d] Contract together matrix elements and perambulators

Table 3.2: computational cost with reference time per gauge configuration and time-slice source to calculate a two point correlation function. N: lattice size, n: rank of distillation basis, T: lattice temporal extent

3.6 Contractions

We must “tie" together the perambulators and elementals with some Dirac gamma structure, where we isolate the channel of interest (J^{PC} continuum quantum numbers) with the lattice group representation. For a single meson correlator, we begin with taking the trace over square matrices, where S is the distillation operator $V(t)JV^{\dagger}(t)$ [28] that acts on the quark fields

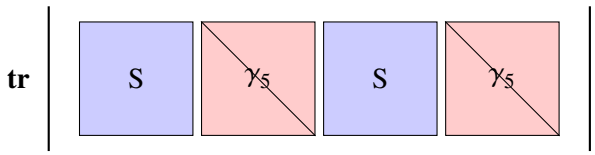

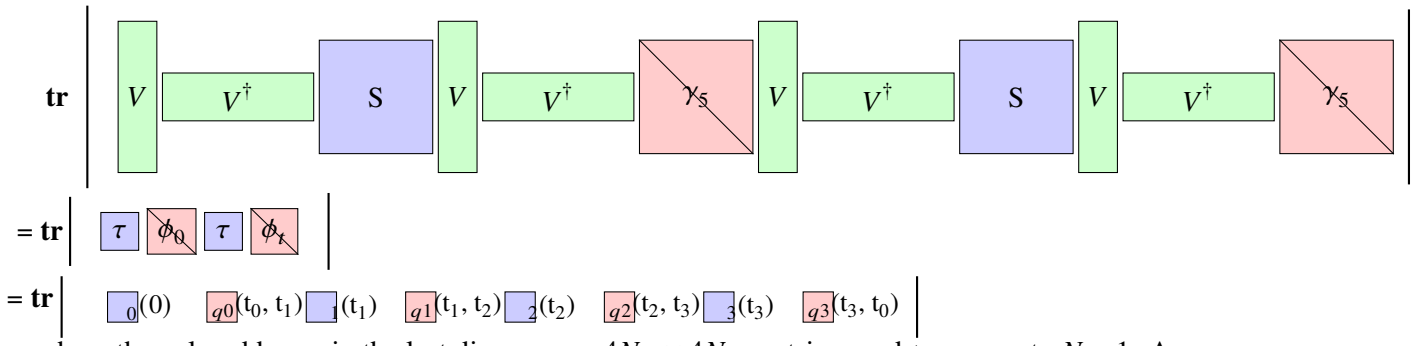

where the colored boxes in the last diagram are $4N_V \times 4N_V$ matrices and t, q go up to $N-1$. A contraction must be carrried out for every gauge configuration (we use 200 in this study); On each configuration, every timeslice and time source is accessed.

3.7 Ensemble Details

We generated ensembles with $N_f = 2+1$ quark flavors, with 6-stout dynamical smeared Wilson fermions and a tree-level Symanzik improved gluon action. Having several a and m_π at our disposal will permit a systematic study of m_π dependence of doubly charmed exotics. Since the doubly charmed tetraquark of interest is close to $D^0 D^0 \pi^+$ threshold, it is sensitive to m_{ud}, thus, it is advantageous to have many ensembles. We are using the action and parameters already employed and tuned for Ref. [29]. We used the ensemble indicated by * to perform this preliminary study, informing the ideal distillation parameters for the remaining ensembles to optimize computational resources.

β	m_{ud}	m_s	$L^3 \times T$	a [fm]	m_π [MeV]	# of traj.
3.7	−0.0200	−0.0	$32^3 \times 96$	0.065	420	2000
3.7*	−0.0220	−0.0	$32^3 \times 96$	0.065	380	2000
3.7	−0.0250	−0.0	$40^3 \times 96$	0.065	300	2000
3.57	−0.0380	−0.007	$24^3 \times 64$	0.085	420	2000
3.57	−0.0440	−0.007	$32^3 \times 64$	0.085	300	2000
3.57	−0.0483	−0.007	$48^3 \times 64$	0.085	200	2000
3.3	−0.1200	−0.057	$16^3 \times 64$	0.125	400	5000
3.3	−0.1233	−0.057	$24^3 \times 64$	0.125	330	5000
3.3	−0.1265	−0.057	$24^3 \times 64$	0.125	280	5000

Table 3.3: Physical parameters of the ensembles that we have available for this project. Bare parameters have been taken from [29].

CHAPTER 4

Interpolating Operators

The overarching aim of hadron spectroscopy on the lattice is to simulate hadrons that we observe in collider experiments. It is advantageous in lattice QCD studies to generate a large basis of interpolating operators to achieve maximal overlap with energy levels of interest. Distillation allows us to restrict this basis to maximize computational efficiency in both the generation of the fundamental objects (perambulators, elementals) and contractions. We first focus on the zero momentum case then extend this framework to non-zero momentum, e.g. mesons in flight. We need to construct operators with the flavor basis $\bar{c}\bar{s}ud$, $c\bar{s}u\bar{d}$, $cc\bar{u}\bar{d}$ and $c\bar{c}u\bar{d}$, which create and destroy a mesonic state, at some fixed time in Euclidean time. The destruction of the state is executed via a contraction of the creation operator with its adjoint at some later time t. The information we can glean from this is the correlation of operators separated by some time t, whereby the transfer matrix eigenstates can be obtained. Moreover, the key difference between lattice and continuum eigenstates is the notion of spin, thus we must work in the circular basis of cartesian-vector-like derivative operators and gamma matrices [30]. Using the preceeding section on correlator function construction from contractions, here we will form local and non-local distilled bilinear operators in different irreps of O_h, which will comprise a $N \times N$ matrix of two-point correlation functions for each irrep, the GEVP. The dimension of this matrix is, not surprisingly, the number of operators constructed in the particular irrep, as we cannot mix operators with different continuum quantum numbers. Our test case will be $J^{PC} = 0^{-+}$, e.g. a pseudoscalar such as the pion. We will walk through lattice operator construction to create a diqaurk $[\bar{q}q]$ of any spin ($J \in \mathbb{Z}$) and parity P with two quark fields and an insertion of the covariant derivative ∇ with gamma structure Γ, the product of which determines the spin J.

4.1 Spin on a cubic lattice

Angular momentum ceases to be a good quantum number on the lattice. Thus, in order to forge a link between continuum spin and spin on the lattice, we must transform lattice operators according to irreps of the cubic group O_h. This optimizes the signal to noise ratio. Only then can we extract eigenstates of the hamiltonian. The lattice irreps, representing symmetries of the cube, are

$$\Lambda = A_1, T_1, T_2, E, A_2 \tag{4.1}$$

Λ	d_Λ	J
A_1	1	$0, 4, 6, \ldots$
A_2	1	$3, 6, 7, \ldots$
E	2	$2, 4, 5, \ldots$
T_1	3	$1, 3, 4, \ldots$
T_2	3	$2, 3, 4, \ldots$

Table 4.1: The table shows the single-valued irreducible representations Λ of the cubic group O, together with their dimensions d_Λ and continuum spin content J.

4.2 Operators on the lattice

A hadronic operator is a functional of the lattice fields with supplied quantum numbers. These are the gauge-invariant color singlet objects. The lattice regulator "breaks" the $SO(3)$ subgroup to a discrete subgroup. $O, \bar{O}$ mapped into the appropriate Hilbert Space such that the corresponding operators $\hat{O}, \hat{O^\dagger}$ annihilate and create the particle states of interest. We can identify physically allowed states via the spectral decomposition of propagators of interpolating operators:

$$\langle O(n_t)\bar{O}(0)\rangle = \sum_n \langle 0|\hat{O}|k\rangle \langle k|\hat{O}^\dagger|0\rangle e^{-n_t a E_k} \tag{4.2}$$

It is important to note that different spin and parity correspond to different gamma matrices in the fermionic bilinears. Armed with the continuum version of operators, which are classified via charge conjugation and Lorentz transformations, we can construct our lattice operators. The first step is to perform a Wick rotation so that our operators now reside in euclidean spacetime, then substitute the covariant derivatives with the lattice covariant derivative [31],

$$\overrightarrow{D}_\mu \psi(x) = \frac{1}{2a}(U_{x,\mu}\psi(x+\hat{\mu}) - U^\dagger_{x-\hat{\mu},\mu}\psi(x-\hat{\mu})) \tag{4.3}$$

4.3 Meson operators at zero total momentum

We detail the operator construction for zero total momentum, continuum spin J^P and spin component m. In general, a local meson interpolator has the form $O_M(n) = \bar{\psi}^{f_1}(n)\Gamma\psi^{f_2}(n)$ where Γ is a monomial of gamma matrices and f are of the exposed flavor indices. In our calculations, the fermions fields $\bar{\psi}, \psi$ are smeared with the distillation operator. The ingredients are gauge-covariant derivatives(for local operators this is just $\mathbb{I}$), Dirac matrix Γ, and the distilled meson elementals and perambulators. We obtain the lattice interpolator from the general(continuum) operator by subducing into irreps of the octahedral group O_h.

Fermion-bilinear operators with continuum spin J and momentum $\vec{p}$ are written like so [10]

$$O^{J,m}(\vec{p},t) = \sum_{\vec{x}} e^{i\vec{p}\vec{x}}\bar{q}(\vec{x},t)[\Gamma\overleftrightarrow{D}\ldots\overleftrightarrow{D}]^{J,m}q(\vec{x},t) \tag{4.4}$$

The simplest interpolating operators are the local fermion bilinears $\bar{\psi}(x)\Gamma\psi(x)$. These are preferred as their corresponding gamma structure is much simpler to implement in the contractions.

Local signifies that the quark fields at the source and sink are not spatially displaced on gauge links. However, the only continuum quantum numbers we can access with local operators are $J^{PC} = 0^{-+}, 0^{++}, 1^{++}, 1^{+-}, 1^{--}$ [32].

For the single pion case, the gamma structure to be inserted between the elementals and perambulators at times t_0, t_f, forming the fermion bilinear are $\gamma_4\gamma_5$ and γ_5.

4.3.1 Distilled Meson Correlator

Consider the following creation/annihilation interpolators for an isovector meson, $\overline{u}\Gamma^A d$ and $\overline{d}\Gamma^B u$, respectively, where Γ is acts on Dirac and color indicies. For smeared quark sources we can write [33]

$$O(x_0,t_0) = \overbrace{\left[\sum_{x_1} S_i^{(t_0,\alpha_0,a_0)}(x_1)^{\alpha_1}_{a_1}\overline{q}^{(f)}(x_1,t)^{\alpha_1}_{a_1}\right]}^{\overline{q}_i(x_0,t)^{\alpha_0}_{a_0}}\Gamma^{\alpha_0\beta_0}\overbrace{\left[\sum_{x_2}(S_k^{(t_0,\beta_0,a_0)}(x_2)^\dagger)^{\alpha_2}_{a_2}q^{(f')}(x_2,t)^{\alpha_2}_{a_2}\right]}^{q_k(x_0,t)^{\beta_0}_{a_0}} \tag{4.5}$$

$$= \overline{q}_i(x_0,t)^{\alpha_0}_{a_0}\Gamma^{\alpha_0\beta_0}q_k(x_0,t)^{\beta_0}_{a_0} \tag{4.6}$$

Let $S = \Box$ and Fourier transform into p-space.

$$\overline{\chi}(p,t) = \overline{u}_w(t)\Box_{wx}(t)\cdot e^{-ip\cdot x}\Gamma^A_{xy}(t)\cdot\Box_{yz}(t)d_z(t) \tag{4.7}$$

Simplifying the notation some (e.g., $\Gamma^A = e^{-ip\cdot x}\Gamma^A_{xy}(t)$), we can express the correlation function as

$$C^{\text{2-pt}}(t',t) = \langle\chi(t)\overline{\chi}(t')\rangle \tag{4.8}$$

$$= \langle\overline{d}(t')\Box(t')\Gamma^B(t')\Box(t')u(t')\cdot\overline{u}(t)\Box(t)\Gamma^A(t)\Box(t)d(t)\rangle \tag{4.9}$$

$$= \text{Tr}\left[\overline{d}(t')V(t')\cdot\underbrace{V^\dagger(t')\Gamma^B V(t')}_{\Phi^B(t')}\cdot V^\dagger(t')u(t')\cdot\overline{u}(t)V(t)\cdot\underbrace{V^\dagger(t)\Gamma^A V(t)}_{\Phi^A(t)}\cdot V^\dagger(t)d(t)\right] \tag{4.10}$$

$$= \text{Tr}\left[\Phi^B(t')\cdot\underbrace{V^\dagger(t')u(t')\overline{u}(t)V(t)}_{\tau_u(t',t)}\cdot\Phi^A(t)\cdot\underbrace{V^\dagger(t)d(t)\overline{d}(t')V(t')}_{\tau_d(t,t')}\right] \tag{4.11}$$

$$= \text{Tr}\left[\Phi^A(t)\tau_u(t',t)\Phi^B(t)\tau_d(t,t')\right] \tag{4.12}$$

Here we have our familiar perambulator with exposed Dirac indices and meson elemental

$$\tau_q(t',t)^{\alpha\beta} = V^\dagger(t')D_q^{-1}(t',t)^{\alpha\beta}V(t) \tag{4.13}$$

$$Phi^{A,\alpha\beta} = V^\dagger(t)(\Gamma^A)^{\alpha\beta}V(t) \tag{4.14}$$

$$= V^\dagger(t)\mathcal{D}^A(t)V(t)\mathcal{S}^{A,\alpha\beta} \tag{4.15}$$

where in the second line we have assumed we can decompose Φ into terms that act only within

coordinate/color space $\mathcal{D}$ or Dirac/spin space $\mathcal{S}$.

Some noteworthy observations are the following:

- Φ has well-defined momentum, whereas there is no momentum projection in the definition of τ
- The choice of source/sink operators is independent of the calculation of τ
- Any source/sink operators can be correlated afterwards once the perambulator has been calculated and stored

It is clear that we can extend this method to determine correlation functions for different, non-degenerate flavors.

4.4 Nonlocal meson operators

To study orbitally excited mesons (higher spin states) we need to employ derivative operators which characterize spatial displacement of quarks on the lattice. These “forward-backward" gauge covariant derivatives allow us to access states with higher angular momentum. On the lattice, these derivatives are finite displacements of quark fields connected by the gauge links. We will include zero, single, and double derivative operators. We must ensure that the operators have definite charge conjugation as well as a projection operator within the corresponding irreps [34]. Our simplest operator, representing a gauge-invariant construction of a quark and antiquark located at different sites on the lattice along some path P is

$$\tilde{\psi}_(x_2)\Pi_P U\Gamma\psi(x_1) \tag{4.16}$$

where Γ takes one of the following forms depending on the state of interest. To access the $J^{PC} = 0^{-+}$ channel, we have a set of three pseudoscalar operators which we can then solve the GEVP for

op.	name	cont.
$\gamma^i\mathbb{B}^i$	$(\rho\times\mathbb{B})_{A_1}$	0^{-+}
$\gamma^4\gamma^i\mathbb{B}^i$	$(\rho_{(2)}\times\mathbb{B})_{A_1}$	0^{-+}
$\gamma^4\gamma^5\gamma^i\nabla^i$	$(b_1\times\nabla)_{A_1}$	0^{-+}

The advantage of employing nonlocal operators is to achieve access to states with nonzero orbital angular momentum. We act on local meson operators with gauge covariant lattice displacements on one (source or sink) or both (source and sink), the smeared quark fields of the discretized theory, to produce nonlocal operators.

4.4.1 Derivative operators

Parallel transport of a lattice field is performed by applying a displacement operator to a quark field. Let $q(x)$ be a quark field and $D_j^{(p)}$ ai displacement operator that moves the quark field for p lattice sites to the direction j in a covariant manner. Let U be the gauge-link as defined in the previous section.

$$D_j^{(p)}q(x) = U_j(x)U_j(x+j)U_j(x+2j)...U_j(x+(p-1)j)q(x+pj) \tag{4.17}$$

with dictionary $x(0), y(1), z(2)$.

Thus, a quark bilinear in its O_h representation is tied together with the spatial path $(x_1 \rightarrow x_2)$. Our new operator will thus live in a representation determined by the Clebsch-Gordan decomposition of the product of representations [35]. The set of operators must have definite charge conjugation and the correct projection operator such that it resides in the proper irrep of the cubic group as dictated by group theory.

Single derivative operators

The general form for single derivative meson operators, in which operators of definite spin can be constructed using the standard $SO(3)$ Clebsch-Gordan coefficients, e.g. for a vector-like gamma matrix and one covariant derivative, operators of $J = 0, 1, 2$ can be formed [36]

$$(\Gamma \times D^{[1]}_{J=1})^{J,M} = \sum_{m_1,m_2} \left\langle 1, m_1; 1, m_2 \middle| J, M \right\rangle \bar{\psi} \Gamma_{m_1} \overleftrightarrow{D}_{m_2} \psi .$$

The choice of Γ plays a role in setting the parity and charge-conjugation quantum numbers of the operator, where the typical naming convention is given by the lowest lying meson in that particular channel. As noted in the introduction of this chapter, we must distribute the different M components belonging to a meson of spin J into definite cubic(lattice) irreps via the group theoretical process called subduction. This is carried out by linear combinations of the M components for each J[36]:

$$O^{[J]}_{\Lambda,\lambda} \equiv (\Gamma \times D^{[n_D]}_{\dots})^{J}_{\Lambda,\lambda} = \sum_{M} \mathcal{S}^{J,M}_{\Lambda,\lambda} \ (\Gamma \times D^{[n_D]}_{\dots})^{J,M} \equiv \sum_{M} \mathcal{S}^{J,M}_{\Lambda,\lambda} O^{J,M},$$

where λ is the "row" of the irrep $(1 \dots \dim(\Lambda))$.

Two derivative operators

Operator	Lattice spatial displacement correspondence
$\gamma_5 \mathbb{D}^i$	$[\gamma_5 * (dydz + dzdy), \gamma_5 * (dzdx + dxdz), \gamma_5 * (dxdy + dydx)]$
$\gamma_4\gamma_5 \mathbb{D}^i$	$[\gamma_5\gamma_4 * (dydz + dzdy), \gamma_5\gamma_4 * (dzdx + dxdz), \gamma_5\gamma_4 * (dxdy + dydx)]$
$\gamma_5 \mathbb{B}^i$	$[\gamma_5 * (dydz + -dzdy), \gamma_5 * (dzdx + -dxdz), \gamma_5 * (dxdy + -dydx)]$
$\gamma_4\gamma_5 \mathbb{B}^i$	$[\gamma_5\gamma_4 * (dydz + -dzdy), \gamma_5\gamma_4 * (dzdx + -dxdz), \gamma_5\gamma_4 * (dxdy + -dydx)]$

Momentum projection

Although we have not yet implemented non-zero momentum into our analysis suite, we very briefly describe what it will entail [37]. For non-local operators used to construct mesons in flight, we must "momentum project" into states of definite momentum, which will reside in some irreducible representation of the octahedral group. We want mesonic states to possess definite spatial momentum on each time slice. Note that it is only necessary to project one of the two interpolators of a correlation function to definite momentum, typically at the sink. $\tilde{O}(\mathbf{p}, n_t) = \frac{1}{\sqrt{\Lambda_3}} \sum_{n \in \Lambda_3} O(\mathbf{n}, nt) e^{-ia\mathbf{np}}$ At non-zero momentum, O_h is broken down to the little groups of Dicyclic nature, e.g. DiC_2, DiC_4. The

extra ingredient required, in contrast to the zero momentum operators, are subduction coefficients that define the helicity operators. For these, we use the Wigner D-matrices then subduce into the irreps of the little group corresponding to the little group of the total momentum $\vec{P}$. See [35],[38] for further information. The crucial piece is that these interpolators for mesons in flight will be put into the GEVP for every relevant irrep.

4.5 Meson-Meson Interpolators

The global $SU(3)$ color symmetry requires that the minimal irreducible color singlet systems can only be $q\bar{q}$, qqq, gg, $q\bar{q}g$ etc., which implies that multi-quark systems can only exist as molecular configurations if there are no other binding mechanisms [39]. Moreover, as a consequence of the $SU(3)^C$ coupling rule, the state $QQ\bar{q}\bar{q}$ has a dimeson configuration as well as a diquark-antidiquark configuration [9][40]. Due to the $SU(3)_c$ coupling rule, when treating tetraquarks as a dimeson system, $(q\bar{q})(q\bar{q})$, the two possible combinations of dimeson $SU(3)_c$ representations that produce a total color singlet state are $(1_c \otimes 1_c)_{1_c}$ and $(8_c \otimes 8_c)_{1_c}$[41]. When the pseudoscalar D and vector D^* are coupled together, the resulting system is DD^* with total angular momentum and parity $J^P = 1^+$. Moreover, the wave function of the tetraquark state T_{cc}^+ includes two color singlet channels:

$$DD^* = \frac{1}{\sqrt{2}}(D^{0*}D^+ - D^+D^*), \tag{4.18}$$

$$D^*D^* = \frac{1}{\sqrt{2}}(D^{*0}D^{*+} - D^{*+}D^{*0}) \tag{4.19}$$

Meson-meson operators are constructed out of single-meson elementals. For mesons in flight, we need to access the helicity operators.

In general, **meson-meson operators** are constructed by forming a product of two single-meson operators with appropriate flavor symmetry: [42]

$$\mathcal{M}^1(x) = M_1(x)M_2^*(x) - M_2(x)M_1^*(x) \tag{4.20}$$

$$M_{1,2}(x) = (l_{1,2})^a_\alpha(x)(\gamma_5)_{\alpha\beta}\bar{\mathcal{Q}}^a_\beta(x) \tag{4.21}$$

$$M^*_{1,2}(x) = (l_{1,2})^a_\alpha(x)(\gamma_i)_{\alpha\beta}\bar{\mathcal{Q}}^a_\beta(x) \tag{4.22}$$

Fermion-bilinear operators with continuum spin J and momentum $\vec{p}$ are written like so [10]

$$\mathcal{O}^{J,m}(\vec{p},t) = \sum_{\vec{x}} e^{i\vec{p}\vec{x}}\bar{q}(\vec{x},t)[\Gamma\overleftrightarrow{D}\dots\overleftrightarrow{D}]^{J,m}q(\vec{x},t) \tag{4.23}$$

ID	$\vec{P}$	LG	Λ^P	J^P	l	interpolators: $M_1(\vec{p}_1^{\,2})M_2(\vec{p}_2^{\,2})$
1	$(0,0,0)$	O_h	T_1^+	1^+	$0,2$	$D(0)D^*(0),\ D(1)D^*(1)\ [2],\ D^*(0)D^*(0)$
2	$(0,0,0)$	O_h	A_1^-	0^-	1	$D(1)D^*(1)$
3	$(0,0,1)\frac{2\pi}{L}$	Dic_4	A_2	$0^-,1^+,2^-$	$0,1,2$	$D(0)D^*(1),\ D(1)D^*(0)$
4	$(1,1,0)\frac{2\pi}{L}$	Dic_2	A_2	$0^-,1^+,2^-,2^+$	$0,1,2$	$D(0)D^*(2),\ D(1)D^*(1)\ [2],\ D(2)D^*(0)$
5	$(0,0,2)\frac{2\pi}{L}$	Dic_4	A_2	$0^-,1^+,2^-$	$0,1,2$	$D(1)D^*(1)$

Figure 4.1: Interpolators along with their total momenta, spatial lattice symmetry group, total spin-parity, and partial wave (of DD^* scattering) that contribute to each irreducible representation

4.5.1 Distilled Meson-Meson Interpolators

First, consider the creation and annihilation interpolators for the $D(0)$ meson with quark content $c\bar{u}$, $\bar{c}u$. For smeared quark sources, we can write [12]

$$O(x_0,t_0) = \left[\sum_{x_1} S_i^{t_0,\alpha_0,a_0}(x_1)_{a_1}^{\alpha_1}\bar{q}^{(f)}(x_1,t)_{a_1}^{\alpha_1}\right]\Gamma^{\alpha_0\beta_0}\left[\sum_{x_2}(S_k^{t_0,\beta_0,a_0}(x_2)^\dagger)_{a_2}^{\alpha_2}\bar{q}^{(f')}(x_2,t)_{a_2}^{\alpha_2}\right] \tag{4.24}$$

$$= \overline{q_i}(x_0,t)_{a_0}^{\alpha_0}\Gamma^{\alpha_0\beta_0}q_k(x_0,t)_{a_0}^{\beta_0} \tag{4.25}$$

Let $S = \square$ and Fourier transform into p-space.

$$\overline{\chi}(p,t) = \overline{u}_w(t)\square_{wx}(t)\cdot e^{-ip\cdot x}\Gamma^A_{xy}(t)\cdot\square_{yz}(t)c_z(t)$$

Simplifying the notation (e.g., $\Gamma^A = e^{-ip\cdot x}\Gamma^A_{xy}(t)$), we can express the correlation function as

$$C^{\text{2-pt}}(t',t) = \langle\chi(t)\overline{\chi}(t')\rangle \tag{4.26}$$

$$= \langle\bar{c}(t')\square(t')\Gamma^B(t')\square(t')u(t')\cdot\overline{u}(t)\square(t)\Gamma^A(t)\square(t)c(t)\rangle \tag{4.27}$$

$$= \mathrm{Tr}\left[\overline{u}(t')V(t')\cdot\underbrace{V^\dagger(t')\Gamma^BV(t')}_{\Phi^B(t')}\cdot V^\dagger(t')c(t')\cdot\bar{c}(t)V(t)\cdot\underbrace{V^\dagger(t)\Gamma^AV(t)}_{\Phi^A(t)}\cdot V^\dagger(t)u(t)\right] \tag{4.28}$$

$$= \mathrm{Tr}\left[\Phi^B(t')\cdot\underbrace{V^\dagger(t')c(t')\bar{c}(t)V(t)}_{\tau_c(t',t)}\cdot\Phi^A(t)\cdot\underbrace{V^\dagger(t)u(t)\overline{u}(t')V(t')}_{\tau_u(t,t')}\right] \tag{4.29}$$

$$= \mathrm{Tr}\left[\Phi^A(t)\tau_u(t',t)\Phi^B(t)\tau_c(t,t')\right] \tag{4.30}$$

Here we have defined the **perambulator** (including Dirac indices)

$$\tau_q(t',t)^{\alpha\beta} = V^\dagger(t')D_q^{-1}(t',t)^{\alpha\beta}V(t) \tag{4.31}$$

as well as elemental Φ

$$\Phi^{A,\alpha\beta} = V^\dagger(t)(\Gamma^A)^{\alpha\beta}V(t) \tag{4.32}$$
$$= V^\dagger(t)\mathcal{D}^A(t)V(t)\mathcal{S}^{A,\alpha\beta} \tag{4.33}$$

where in the second line we have assumed we can decompose Φ into terms that act only within coordinate/color space $\mathcal{D}$ or Dirac spin space $\mathcal{S}$.

Distilled Meson-Meson Correlators

Wick's theorem says that a correlation function is given by the sum of all possible pairs of quark contractions, specifically batched tensor contractions. Given a dimeson operator $[MM']$, we have the following spectral decomposition:

$$\langle [MM'](t)[MM']^\dagger(0)\rangle = \sum_n |Z^{(n)}_{MM'}|^2 e^{-E^{(n)}_{MM'}t} \tag{4.34}$$

As described in the chapter on operator construction, we can form a set of N MM' interpolating operators

$$\{[MM']^{(0)}, \ldots, [MM']^{(N)}\}$$

which have non-trivial overlap with the mesonic state of interest MM'. The question is thus, how does one determine the magnitude of the overlaps with the state of interest? Conveniently, the outer product of the set of N interpolating operators acting on itself creates a $N \times N$ matrix of MM' correlators. Not surprisingly, these share the same spectrum.

In theory, one could fit all $N \times N$ correlators using a simultaneous fit, however, at this point it is standard practice to solve the generalized eigenvalue problem for the set of correlation functions. Solving the following for the eigenvectors $v_n(t, t_0)$ gives us an optimized operator basis

$$C(t)v_n(t, t_0) = \lambda_n(t, t_0)C(t_0)v_n(t, t_0) \tag{4.35}$$

Instead of solving the GEVP at the operator level, we deal with the correlation functions directly to yield the optimized correlators

$$\langle [MM'](t)[MM']^\dagger(0)\rangle = \sum_n |Z^{(n)}_{MM'}|^2 e^{-E^{(n)}_{MM'}t} \tag{4.36}$$

CHAPTER 5

Mesonic Signal Saturation

The meson mass spectrum is extracted via Bayesian analysis of two-point correlation functions. One can systematically improve lattice simulations by using more statistics and employing a collection of ensembles with various quark mass values and lattice spacings. Ultimately, the continuum masses are what we are after. We strive for good continuum limits by using many lattice spacings. We perform a study of the resulting mesonic correlator signal using various distillation parameters to determine the optimal parameters to use. In particular, we want to test the optimal size of the eigenvector basis used to generate our perambulators and elementals, as well as the number of source locations per configuration in order to obtain a good signal while keeping the computational cost contained.

Given an operator with pion quantum numbers, such as $\phi_L(x) = \bar{d}(x)\gamma_5 u(x)$ or some smeared version of this, denoted $\phi_S(x)$, the dimensionless correlator from Euclidean time t_i to Euclidean time t_f with momentum $\vec{p}$ is

$$\Gamma^{\pi\pi}_{AB}(t_i, t_f, \vec{p}) \quad = \quad a^6 \sum_{\vec{x}_f} e^{-i(\vec{x}_f - \vec{x}_i)\cdot\vec{p}} \left\langle 0 \left| \phi_B(x_f) \phi^\dagger_A(x_i) \right| 0 \right\rangle \tag{5.1}$$

Here we present results for a systematic study of how the signal of the pion two-point correlator with $\vec{p} = (0, 0, 0)$ at zero displacement is affected by the rank of the distillation basis (number of eigenvectors used n_{vec}) and the number of t_{src} insertions. The rank of the distillation basis take values in the set $n_{vec} \in 32, 64, 96, 128$ and the number of $t_{src} \in 1, 2, 4, 8, 12, 24$. We perform this study on the ensemble $\beta = 3.7$, $m_{ud} = -0.0220$, $m_s = -0.0$, $L^3 \times T = 32^3 \times 96$. This determination will allow us to optimize compute resources for the eigenbasis, perambulators, and elementals for the rest of the ensembles we have generated. We chose the pion as a test case as it typically provides the cleanest signal in lattice calculations. With this complete, we will proceed with computing the fundamental distillation objects using a distillation basis of rank 96 and 24 t_{src} insertions for the perambulators. We are currently investigating potential systematic errors or underestimation of statistical uncertainties with regards to the impact of the number of t_{src} insertions on the pion mass. The following two figures highlight the results that prompted this investigation, as in theory, they should all agree within relative errors.

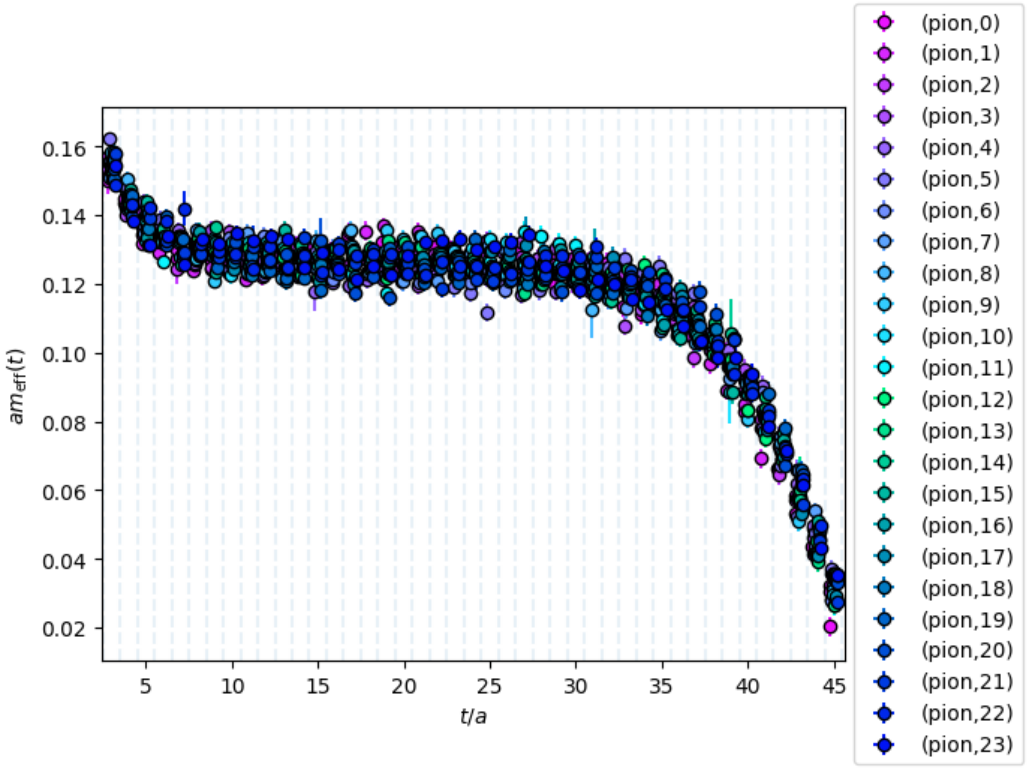

Figure 5.1: Effective mass plot of pion correlators for each t_{src} insertion after shifting all to the origin.

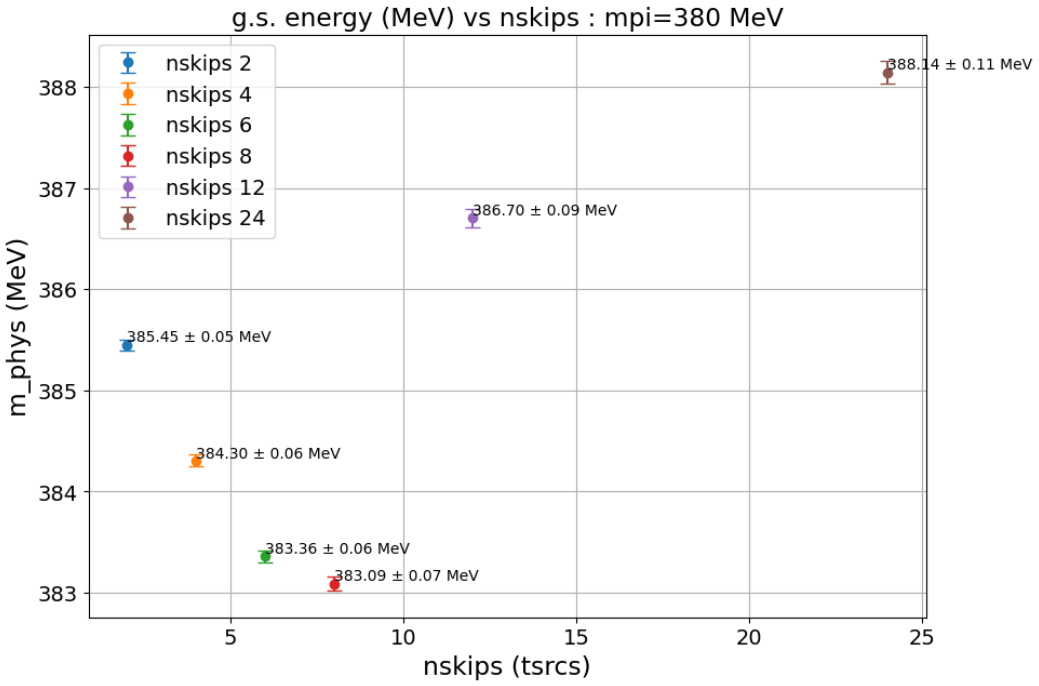

Figure 5.2: Comparison of ground state energy of the pion for various numbers of t_{src} insertions.

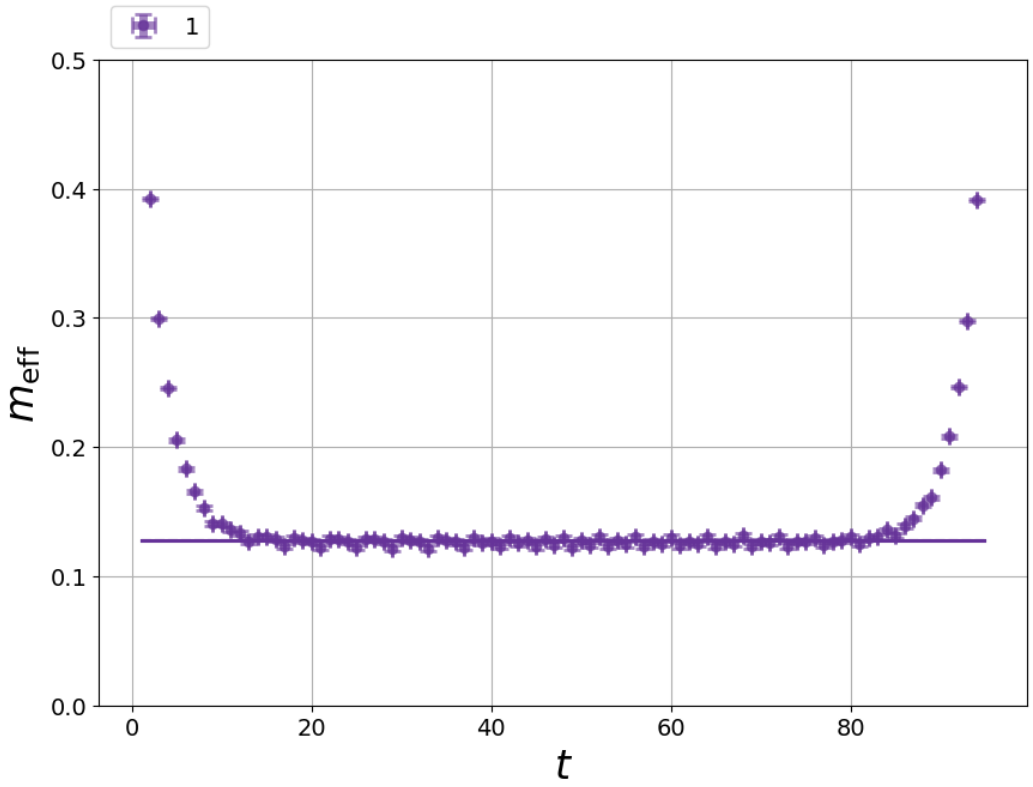

Figure 5.3: Single state fit to the effective mass of the pion for 24 t_{src} insertions.

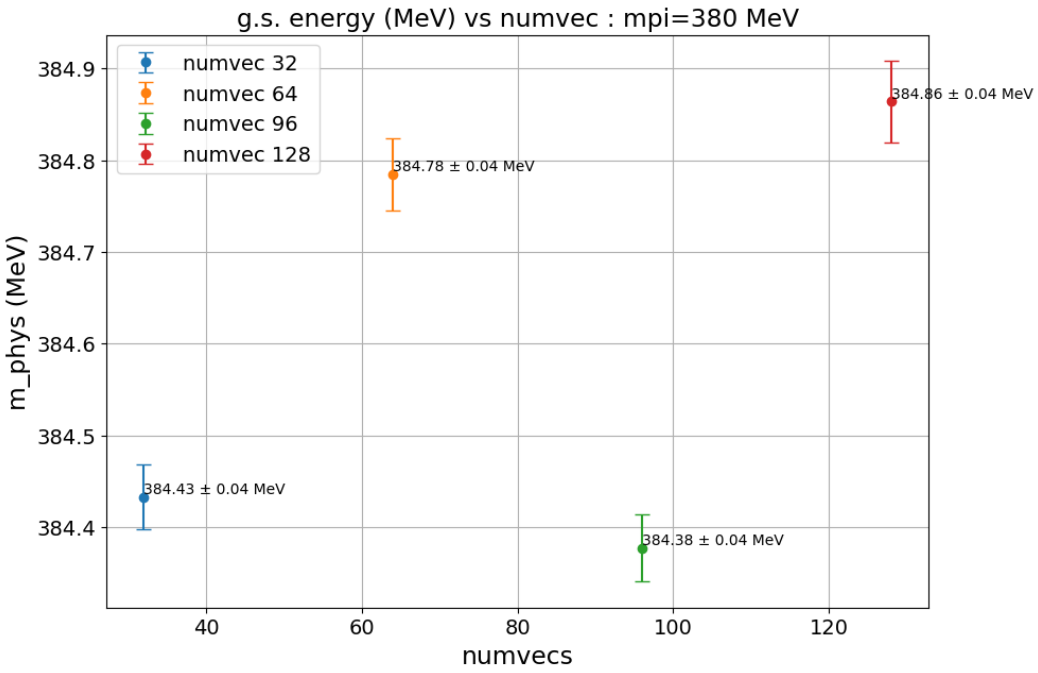

Figure 5.4: Comparison of ground state energy of the pion for different sizes (rank) of the distillation basis.

CHAPTER 6

Conclusion

6.1 Outlook: Towards the Quark Mass Dependence of $T_{cc}(3875)$

In this section we briefly describe the remaining tasks and the end goals of this project which will comprise a Doctoral thesis. We endeavor to perform a rigorous analysis of the dependence of energy spectra and scattering phase shifts on the degree of distillation smearing. Our testing ground will be the single and double pion system for a collection of covariant derivatives and total momenta. This analysis for hadrons containing charm quarks will then follow suit. In this vein, the remaining tasks are

- computation of meson and doubly charmed spectrum for a range of center-of-mass momenta in various irreps of O_h
- Finite volume analysis of the discrete spectrum on several volumes and momentum frames
- Extract isospin-1 P-wave scattering phase shift
- Determine the systematic uncertainty coming from m_π
- T_{cc}^+ dependence on m_π as the latter approaches the physical point

Hadrons containing heavy quarks are prone to discretization errors thus a controlled continuum limit at finite lattice spacing is required!

6.1.1 Exotic Hadrons in a (very small) nutshell

Since the turn of the century, collider experiments have identified resonances that do not fit into the traditional quark model; The two competing hypotheses are that these states are either bound states of di-quarks and anti-di-quarks (tetraquarks) or di-meson states. For comprehensive reviews the topic, see [43][41] [9]We aim to confirm that the doubly charmed tetraquark state of interest is a member of the class of hadrons shown in g

The particular color structure of a tetraquark that we will investigate is the hadronic molecule type

$$3_q \otimes 3_q \otimes \bar{3}_{\bar{q}} \otimes \bar{3}_{\bar{q}} \rightarrow 1_{[\bar{q}q]_1[\bar{q}q]_1} \rightarrow \delta_{ab}\delta_{cd} \times \bar{q}^a q^b \bar{q}^c q^d \tag{6.1}$$

Where $a..d = 1..3$ and $n = 1...8$ are the color indices.

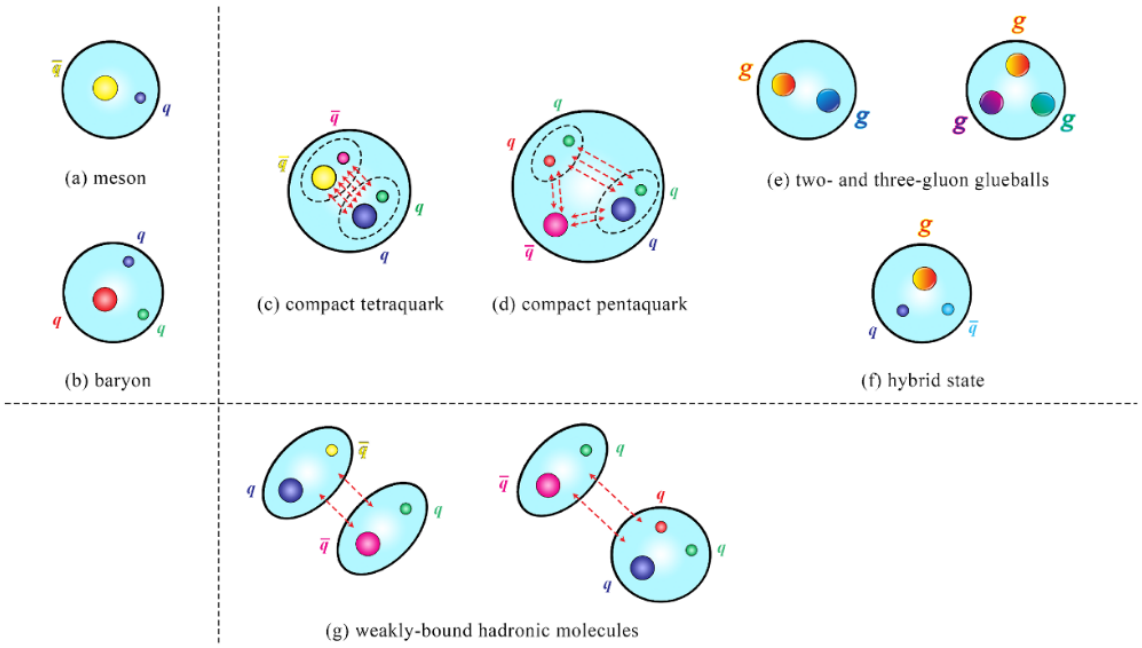

Figure 6.1: different structures of hadrons with emphasis on the di-meson state in (g) and the tetraquark state in (c)

The flavor $SU(3)$ representations of the tetraquark states are [44]

$$\begin{aligned} &3_q \otimes 3_q \otimes \bar{3}_{\bar{q}} \otimes \bar{3}_{\bar{q}} \\ &= (1 \oplus 8)_{[qq]_{\bar{3}}[\bar{q}\bar{q}]_3} \oplus (8 \oplus 10)_{[qq]_6[\bar{q}\bar{q}]_3} \\ &\oplus (8 \oplus \bar{10})_{[qq]_{\bar{3}}[\bar{q}\bar{q}]_{\bar{6}}} \oplus (1 \oplus 8 \oplus 27)_{[qq]_6[\bar{q}\bar{q}]_{\bar{6}}} \end{aligned} \tag{6.2}$$

6.2 Conclusion

Our goal with this project is to better understand the exotic doubly charmed sector using a data-driven approach with LQCD and distillation in an attempt to dispel disagreement that currently exists in the experimental literature. In Chapter 2 we laid out the formalism for discretizing the continuum theory of QCD and how we transcribe this onto a computer such that we can compute Euclidean correlation functions on all possible gauge field configurations. We motivated our use of distillation smearing with an explanation of traditional quark field smearing methods; This will allow us to efficiently compute the necessary elements for performing hadron spectroscopy calculations, in the form of tensor contractions, while keeping the computational cost low. We laid out the computational considerations of our lattice setup in Chapter 3 and the required software stack to compute eigenpairs, meson elementals, and perambulators using distillation. We highlighted the cost and storage of this method and diagrammatically showed the layout of contracting distilled objects on the lattice to extract physical observables. The construction of a sufficiently large basis of interpolating operators to maximize overlap with energy levels of interest was outlined in Chapter 4. This requires both zero and

non-zero values of total momentum and several levels of displacement to access all the spin channels in the continuum. In Chapter 5 we presented our preliminary study on mesonic signal saturation with distillation in order to pin down the optimal parameters to use for the remainder of the ensembles we have at our disposal, namely the rank of the distillation basis and the number of t_{src} insertions. Based on this study, we will generate the rest of our objects using a distillation basis size of 96 and 24 source insertions. Ultimately, this setup will allow us to access the doubly charmed sector and construct di-meson states to extract scattering amplitudes to further probe XYZ states, see the Introduction chapter, with LQCD.

APPENDIX A

Appendix

A.1 Group theory in QCD

We briefly touch on the pertinent group theory that manifests in the study of QCD and how this relates to operator construction on the lattice. There exists 8 unique diquark multiplets (flavor × color × spin) that can be created from the vacuum by operators biliner in the quark field. Each quark is a color triplet, therefor ethe pair of them can form a color $\bar{3}c$, which is antisymmetiric, or the symmetric 6_c. This is due to the fact that each flavor of quark belongs to the fundamental representation 3 and contains a triplet of fields,

$$\Psi = \begin{bmatrix} \psi_1 \\ \psi_2 \\ \psi_3 \end{bmatrix} \tag{A.1}$$

We obtain the stationary state energies of QCD using periodic boundary conditions by working in a cubic box. However, we no longer have the full rotational symmetry of the continuum. The lattice breaks rotational symmetry due to the fact that the spatial volume of the hypercube possess only discrete rotational symmetry, that of a cube, so we can think of this as a subgroup of the full rotational symmetry in the continuum. Consequently, these stationary states can no longer be labelled by the typical spin-J quantum numbers. Thus, we need a "new" quantum number. The group theory machinery to obtain these new quantum numbers are the irreps of the cubic space group. **The interpolating operators used in a lattice calculation must transform irreducibly under all symmetries of the 3D-cubic lattice**.

Irreducible representations(irreps) of the discrete rotational symmetry of the spatial volume of our 4D hypercube (the lattice) are members of the little group O_h. Thus, we must use a scheme to map the continuum spin quantum number eg. $J = 0, 1, 2, \ldots$ to the notion of spin on the lattice where the correspondence is [36]

The input data one needs to provide in order to obtain the correct little group (L), and thus the corresponding "shells", is

$$O_h, P \rightarrow L \tag{A.2}$$

$$\{l\vec{k}, \forall l \in L\} \tag{A.3}$$

J	irreps
0	$A_1(1)$
1	$T_1(3)$
2	$T_2(3) \oplus E(2)$
3	$T_1(3) \oplus T_2(3) \oplus A_2(1)$
4	$A_1(1) \oplus T_1(3) \oplus T_2(3) \oplus E(2)$

Table A.1: Continuum spins subduced into lattice irreps $\Lambda(\dim)$.

Where l is a 3×3 matrix and P is total momenta. This satisfies the relation $l\,|k_1\rangle = |k_2\rangle$ and leads to the more general relation

$$\langle k_i|l|k_j\rangle = (M_l)_{ij} \tag{A.4}$$

Where M_l is a permutation matrix which is a reducible representation of L and has the dimensions $|\text{shell}| \times |\text{shell}|$. For example,

$$k^2 = 0\vec{k} = 000 \qquad (000) \tag{A.5}$$

$$k^2 = 1\vec{k} = 100 \qquad (100), (-100)(010)(0-10)(001)(00-1) \tag{A.6}$$

$$\tag{A.7}$$

so we have a total of six possible momenta 3-tuples corresponding to total momenta $k^2 = 1$. We can proceed in the same fashion to obtain 12 for $k^2 = 2$, 8 for $k^2 = 3$, and 24 for $k^2 = 5$.

A.2 Gamma matrices

Gamma matrices generate a representation of the Clifford algebra $C\updownarrow_{1,3}\mathbb{R}$ and satisfy the anticommutation relation

$$\{\gamma^\mu, \gamma^\nu\} = 2\eta^{\mu,\nu} \tag{A.8}$$

A.2.1 `Chroma` Euclidean Dirac Matrices

$$\gamma_0 = \begin{bmatrix} 0 & 0 & -1 & 0 \\ 0 & 0 & 0 & -1 \\ -1 & 0 & 0 & 0 \\ 0 & -1 & 0 & 0 \end{bmatrix}$$

$$\gamma_1 = \begin{bmatrix} 0 & 0 & 0 & -i \\ 0 & 0 & -i & 0 \\ 0 & i & 0 & 0 \\ i & 0 & 0 & 0 \end{bmatrix}$$

n_Γ(dec)	n_Γ(bin)	name	Γ	state	$\widetilde{n_\Gamma}$(dec)
0	0000	a0	1	a_0	15
1	0001	rho_x	γ_1	$\rho(x)$	14
2	0010	rho_y	γ_2	$\rho(y)$	13
3	0011	b1_z	$\gamma_1\gamma_2$	$b_1(z)$	12
4	0100	rho_z	γ_3	$\rho(z)$	11
5	0101	b1_y	$\gamma_1\gamma_3$	$-b_1(y)$	10
6	0110	b1_x	$\gamma_2\gamma_3$	$b_1(x)$	9
7	0111	pion_2	$\gamma_1\gamma_2\gamma_3 = \gamma_5\gamma_4$	π	8
8	1000	b0	γ_4	b_0	7
9	1001	rho_x_2	$\gamma_1\gamma_4$	$\varrho(x)$	6
10	1010	rho_y_2	$\gamma_2\gamma_4$	$\varrho(y)$	5
11	1011	a1_z	$\gamma_1\gamma_2\gamma_4 = \gamma_3\gamma_5$	$a_1(z)$	4
12	1100	rho_z_2	$\gamma_3\gamma_4$	$\varrho(z)$	3
13	1101	a1_y	$\gamma_1\gamma_3\gamma_4 = -\gamma_2\gamma_5$	$-a_1(y)$	2
14	1110	a1_x	$\gamma_2\gamma_3\gamma_4 = \gamma_1\gamma_5$	$a_1(x)$	1
15	1111	pion	$\gamma_1\gamma_2\gamma_3\gamma_4 = \gamma_5$	π	0

$$\gamma_2 = \begin{bmatrix} 0 & 0 & 0 & -1 \\ 0 & 0 & 1 & 0 \\ 0 & 1 & 0 & 0 \\ -1 & 0 & 0 & 0 \end{bmatrix}$$

$$\gamma_3 = \begin{bmatrix} 0 & 0 & -i & 0 \\ 0 & 0 & 0 & i \\ i & 0 & 0 & 0 \\ 0 & -i & 0 & 0 \end{bmatrix}$$

$$\gamma_4 = -\gamma_0$$

$$\gamma_5 = \gamma_0\gamma_1\gamma_2\gamma_3 = \begin{bmatrix} 1 & 0 & 0 & 0 \\ 0 & 1 & 0 & 0 \\ 0 & 0 & -1 & 0 \\ 0 & 0 & 0 & -1 \end{bmatrix}$$

$$C = -\gamma_0\gamma_2$$

`Chroma` uses the following conventions [22] For particles of spin-1 can *arbitrarily* define a sign convention:

$$\begin{aligned} \rho(k) &\equiv \bar{\psi}\gamma_k\psi \\ \varrho(k) &\equiv \bar{\psi}\gamma_k\gamma_4\psi \\ a_1(k) &\equiv \bar{\psi}\gamma_k\gamma_5\psi \\ b_1(k) &\equiv \bar{\psi}\tfrac{1}{2}\epsilon_{ijk}\gamma_i\gamma_j\psi \end{aligned}$$

With this convention some of the chroma gamma matrices carry a minus sign when creating a state.

Bibliography

[1] F. Knechtli, M. Gnther and M. Peardon,
Lattice Quantum Chromodynamics: Practical Essentials, 1st,
Springer Publishing Company, Incorporated, 2016, ISBN: 9402409971 (cit. on pp. 1, 12, 18).

[2] R. Gupta, *Introduction to Lattice QCD*, (1998), arXiv: hep-lat/9807028 [hep-lat],
URL: https://arxiv.org/abs/hep-lat/9807028 (cit. on p. 1).

[3] C. Gattringer and C. B. Lang,
Quantum Chromodynamics on the Lattice: An Introductory Presentation, (2009),
URL: https://api.semanticscholar.org/CorpusID:117994235 (cit. on p. 1).

[4] D. Griffiths, *Introduction to Elementary Particles*, (1987) (cit. on p. 1).

[5] T. P. Cheng, L.-F. Li and D. A. Gross, "Gauge Theory of elementary particle physics", 1984,
URL: https://api.semanticscholar.org/CorpusID:119854624 (cit. on pp. 1, 4).

[6] M. Gell-Mann, *A Schematic Model of Baryons and Mesons*, Phys. Lett. **8** (1964) 214
(cit. on pp. 1, 3).

[7] G. Zweig, *An SU(3) model for strong interaction symmetry and its breaking. Version 1*, (1964)
(cit. on p. 1).

[8] M. Y. Han and Y. Nambu, *Three Triplet Model with Double SU(3) Symmetry*,
(1965), ed. by T. Eguchi (cit. on p. 1).

[9] N. Brambilla et al., *The XYZ states: experimental and theoretical status and perspectives*,
Phys. Rept. **873** (2020) 1, arXiv: 1907.07583 [hep-ex] (cit. on pp. 1, 28, 35).

[10] G. K. C. Cheung, C. E. Thomas, J. J. Dudek and R. G. Edwards,
Tetraquark operators in lattice QCD and exotic flavour states in the charm sector,
Journal of High Energy Physics **2017** (2017), ISSN: 1029-8479,
URL: http://dx.doi.org/10.1007/JHEP11(2017)033 (cit. on pp. 1, 24, 28).

[11] R. Aaij et al., *Observation of an exotic narrow doubly charmed tetraquark*,
Nature Phys. **18** (2022) 751, arXiv: 2109.01038 [hep-ex] (cit. on p. 2).

[12] M. Peardon et al.,
A novel quark-field creation operator construction for hadronic physics in lattice QCD, en,
Physical Review D **80** (2009) 054506, arXiv:0905.2160 [hep-lat], ISSN: 1550-7998, 1550-2368,
URL: http://arxiv.org/abs/0905.2160 (visited on 23/07/2024)
(cit. on pp. 3, 11, 12, 19, 29).

[13] D. J. Gross and F. Wilczek, *Asymptotically Free Gauge Theories. I*, (1973), URL: https://link.aps.org/doi/10.1103/PhysRevD.8.3633 (cit. on p. 3).

[14] S. Weinberg, *Non-Abelian Gauge Theories of the Strong Interactions*, Phys. Rev. Lett. (1973), URL: https://link.aps.org/doi/10.1103/PhysRevLett.31.494 (cit. on p. 3).

[15] K. G. Wilson, *Confinement of Quarks*, Phys. Rev. D (1974) (cit. on pp. 4, 7).

[16] B. C. Hall, *Lie Groups, Lie Algebras, and Representations: An Elementary Introduction*, (2004), URL: https://api.semanticscholar.org/CorpusID:118901542 (cit. on p. 9).

[17] C. Morningstar and M. Peardon, *Analytic smearing of* SU(3) *link variables in lattice QCD*, Phys. Rev. D **69** (5 2004) 054501, URL: https://link.aps.org/doi/10.1103/PhysRevD.69.054501 (cit. on p. 12).

[18] I. Montvay and G. Münster, *Quantum Fields on a Lattice*, Cambridge Monographs on Mathematical Physics, Cambridge University Press, 1994 (cit. on p. 16).

[19] M. Luscher, "Computational Strategies in Lattice QCD", *Les Houches Summer School: Session 93: Modern perspectives in lattice QCD: Quantum field theory and high performance computing*, 2010 331, arXiv: 1002.4232 [hep-lat] (cit. on p. 16).

[20] M. Creutz, *Global Monte Carlo algorithms for many-fermion systems*, Phys. Rev. D **38** (1988) 1228 (cit. on p. 16).

[21] J. Finkenrath, *Review on Algorithms for dynamical fermions*, PoS **LATTICE2022** (2023) 227, eprint: 2402.11704 (cit. on p. 16).

[22] R. G. Edwards and B. Joó, *The Chroma Software System for Lattice QCD*, Nuclear Physics B - Proceedings Supplements **140** (2005) 832, ISSN: 0920-5632, URL: http://dx.doi.org/10.1016/j.nuclphysbps.2004.11.254 (cit. on pp. 17, 18, 41).

[23] E. Romero and K. Orginos, *Efficient computation of baryon interpolating fields in Lattice QCD*, arXiv:2011.10571 [hep-lat], 2020, URL: http://arxiv.org/abs/2011.10571 (visited on 26/03/2024) (cit. on pp. 18, 19).

[24] A. Stathopoulos and J. R. McCombs, *PRIMME: PReconditioned Iterative MultiMethod Eigensolver: Methods and software description*, ACM Transactions on Mathematical Software **37** (2010) 21:1 (cit. on p. 18).

[25] A. Frommer et al., *A multigrid accelerated eigensolver for the Hermitian Wilson–Dirac operator in lattice QCD*, Comput. Phys. Commun. **258** (2021) 107615, arXiv: 2004.08146 [hep-lat] (cit. on p. 18).

[26] E. D. Napoli, D. Fabregat-Traver, G. Quintana-Ortì and P. Bientinesi, *Towards an Efficient Use of the BLAS Library for Multilinear Tensor Contractions*, (2013), eprint: 1307.2100, URL: https://arxiv.org/abs/1307.2100 (cit. on p. 19).

[27] M. Clark et al., *Accelerating Lattice QCD Multigrid on GPUs Using Fine-Grained Parallelization*, (2016) (cit. on p. 20).

[28] J. Neuendorf et al., *Optimized Distillation Profiles for Heavy-Light Spectroscopy*, (2024), arXiv: 2401.05828 [hep-lat] (cit. on p. 20).

[29] S. Durr et al., *Ab-Initio Determination of Light Hadron Masses*, Science **322** (2008) 1224, arXiv: 0906.3599 [hep-lat] (cit. on p. 21).

[30] C. Morningstar et al., *Extended hadron and two-hadron operators of definite momentum for spectrum calculations in lattice QCD*, Phys. Rev. D **88** (2013) 014511, arXiv: 1303.6816 [hep-lat] (cit. on p. 23).

[31] M. Göckeler et al., *Perturbative renormalization of lattice bilinear quark operators*, (1996) (cit. on p. 24).

[32] J. J. Dudek, R. G. Edwards, N. Mathur and D. G. Richards, *Charmonium excited state spectrum in lattice QCD*, Physical Review D **77** (2008), ISSN: 1550-2368, URL: http://dx.doi.org/10.1103/PhysRevD.77.034501 (cit. on p. 25).

[33] G. Cheung, *Spectroscopy of exotic charm mesons from lattice QCD*, PhD thesis: Cambridge U., DAMTP, 2019 (cit. on p. 25).

[34] X. Liao and T. Manke, *Excited charmonium spectrum from anisotropic lattices*, (2002), arXiv: hep-lat/0210030 [hep-lat], URL: https://arxiv.org/abs/hep-lat/0210030 (cit. on p. 26).

[35] S. Basak et al., *Clebsch-Gordan construction of lattice interpolated fields for excited baryons*, Physical Review D **72** (2005), ISSN: 1550-2368, URL: http://dx.doi.org/10.1103/PhysRevD.72.074501 (cit. on pp. 27, 28).

[36] J. J. Dudek, R. G. Edwards, M. J. Peardon, D. G. Richards and C. E. Thomas, *Toward the excited meson spectrum of dynamical QCD*, Physical Review D **82** (2010), ISSN: 1550-2368, URL: http://dx.doi.org/10.1103/PhysRevD.82.034508 (cit. on pp. 27, 39).

[37] Martin Ueding, *Three Pion Scattering at Maximal Isospin from Lattice QCD at Physical Mass*, In this work the scattering of two pions in $I = 2$ and three pions in $I = 3$ is analyzed with lattice QCD. The process is computed on three Wilson clover twisted mass ensembles generated by the ETMC with total momentum up to $vecP^2leq4$ in all irreducible representations. One ensemble has been simulated at the physical pion mass. The correlation functions are treated with methods to suppress thermal states and excited states. Energy extraction is performed with multiple different fit methods and a combination afterwards such that the systematic errors from fit range selection are taken into account. The three-pion spectrum has been fitted using the RFT approach. We obtain $a_0M_piup = 0.0481(86)$ for the two-pion scattering length at the physical pion mass. In the three-pion sector a constant and linear coefficient of the contact interaction has been extracted. The constant term agrees both with an existing analysis and leading order ChPT, the linear term has tension with the leading order ChPT prediction at high pion masses., PhD thesis: Rheinische Friedrich-Wilhelms-Universität Bonn, 2021, URL: https://hdl.handle.net/20.500.11811/8872 (cit. on p. 27).

[38] C. Morningstar et al., *Extended hadron and two-hadron operators of definite momentum for spectrum calculations in lattice QCD*, en,
Physical Review D **88** (2013) 014511, arXiv:1303.6816 [hep-lat], ISSN: 1550-7998, 1550-2368,
URL: http://arxiv.org/abs/1303.6816 (visited on 30/09/2024) (cit. on p. 28).

[39] M. Abolnikov et al., *Internal structure of the $T_{cc}(3875)^+$ from its light-quark mass dependence*, (2024), arXiv: 2407.04649 [hep-ph] (cit. on p. 28).

[40] M. Padmanath and S. Prelovsek,
Signature of a Doubly Charm Tetraquark Pole in DD Scattering on the Lattice*,
Physical Review Letters **129** (2022), ISSN: 1079-7114,
URL: http://dx.doi.org/10.1103/PhysRevLett.129.032002 (cit. on p. 28).

[41] F.-K. Guo et al., *Hadronic molecules*, (2018), eprint: 1705.00141 (cit. on pp. 28, 35).

[42] P. Junnarkar, N. Mathur and M. Padmanath, *Study of doubly heavy tetraquarks in lattice QCD*,
Physical Review D **99** (2019), ISSN: 2470-0029,
URL: http://dx.doi.org/10.1103/PhysRevD.99.034507 (cit. on p. 28).

[43] H.-X. C. et al, *An updated review of the new hadron states*, Rep. Prog. Phys. **86** (2023) (cit. on p. 35).

[44] H. Huang, C. Deng, X. Liu, Y. Tan and J. Ping,
Tetraquarks and Pentaquarks from Quark Model Perspective, (2023) (cit. on p. 36).

List of Figures

3.1 Flowchart of the computational workflow for computing lattice objects with distillation. 17

4.1 Interpolators along with their total momenta, spatial lattice symmetry group, total spin-parity, and partial wave (of DD^* scattering) that contribute to each irreducible representation 29

5.1 Effective mass plot of pion correlators for each t_{tsrc} insertion after shifting all to the origin. 32
5.2 Comparison of ground state energy of the pion for various numbers of t_{src} insertions. 32
5.3 Single state fit to the effective mass of the pion for 24 t_{src} insertions. 33
5.4 Comparison of ground state energy of the pion for different sizes (rank) of the distillation basis. 34

6.1 different structures of hadrons with emphasis on the di-meson state in (g) and the tetraquark state in (c) 36

List of Tables

3.1 The tensor structure of `Chroma` objects. `Nd`: num. space-time dimensions, `Nc`: dimension of the color vector space, `Ns`: dimension of the spin vector space. [22] . . 18

3.2 computational cost with reference time per gauge configuration and time-slice source to calculate a two point correlation function. N: lattice size, n: rank of distillation basis, T: lattice temporal extent 20

3.3 Physical parameters of the ensembles that we have available for this project. Bare parameters have been taken from [29]. 21

4.1 The table shows the single-valued irreducible representations Λ of the cubic group O, together with their dimensions d_Λ and continuum spin content J. 24

A.1 Continuum spins subduced into lattice irreps $\Lambda(\dim)$. 40